Published in final edited form as:
J Mol Biol. 2008 March 14; 377(1): 9–27.

Formation of A Wrapped DNA-Protein Interface: Expermental Characterization and Analysis of the Large Contributions of Ions and Water to the Thermodynamics of Binding IHF to H′DNA

Kirk A. Vander Meulen[1], **Ruth M. Saecker**[2], and **M. Thomas Record Jr.**[1,2,*]

1 *Department of Biochemistry, University of Wisconsin, Madison WI 53706*

2 *Department of Chemistry, University of Wisconsin, Madison WI 53706*

Abstract

To characterize driving forces and driven processes in formation of a large-interface, wrapped protein-DNA complex analogous to the nucleosome, we have investigated the thermodynamics of binding the 34 bp H′ DNA sequence to the *E. coli* DNA-remodeling protein Integration Host Factor (IHF). Isothermal titration calorimetry (ITC) and fluorescence resonance energy transfer (FRET) are applied to determine effects of salt concentration (KCl, KF, KGlutamate (KGlu)), and of the excluded solute glycine betaine, on the binding thermodynamics at 20°C. Both the binding constant K_{obs} and enthalpy $\Delta H°_{obs}$ depend strongly on [salt] and anion identity. Formation of the wrapped complex is enthalpy-driven, especially at low [salt] (e.g. $\Delta H°_{obs} = -20.2$ kcal $\cdot$ mol^{-1} in 0.04 M KCl). $\Delta H°_{obs}$ increases linearly with [salt] with a slope ($d\Delta H°_{obs}/d$[salt]) which is much larger in KCl (38 ± 3 kcal $\cdot$ mol^{-1}M^{-1}) than in KF or KGlu (average 11 ± 2 kcal $\cdot$ mol^{-1}M^{-1}). At 0.33 M [salt], K_{obs} is approximately 30-fold larger in KGlu or KF than in KCl, and the [salt] derivative $SK_{obs} = d\ln K_{obs}/d\ln$[salt] is almost twice as large in magnitude in KCl (−8.8 ± 0.7) as in KF or KGlu (average −4.7 ± 0.6).

A novel analysis of the large effects of anion identity on K_{obs}, SK_{obs} and on $\Delta H°_{obs}$ dissects coulombic, Hofmeister and osmotic contributions to these quantities. This analysis attributes anion-specific differences in K_{obs}, SK_{obs} and $\Delta H°_{obs}$ to (i) displacement of a large number of waters of hydration (estimated to be 1.0 (± 0.2) × 10^3) from the 5340 Å^2 of IHF and H′ DNA surface buried in complex formation, and (ii) significant local exclusion of F^- and Glu^- from this hydration water, relative to the situation with Cl^-, which we propose is randomly distributed. To quantify net water release from anionic surface (22% of the surface buried in complexation, mostly from DNA phosphates), we determined the stabilizing effect of glycine betaine (GB) on K_{obs}: $d\ln K_{obs}/d$[GB] = 2.7 ± 0.4 at constant KCl activity, indicating the net release of 150 H_2O from anionic surface.

Introduction

The crystal structure of the specific complex of E. coli Integration Host Factor (IHF), a relatively small (22 kDa) heterodimer, with the 34 base pair (bp) DNA sequence of the H′ site from bacteriophage λ reveals that H′ DNA is sharply bent and wrapped in a “U-turn” about the arms and body of IHF (Figure 1A).[1] This structure eloquently illustrates the role of specific

*corresponding author: 433 Babcock Drive, Madison, WI 53706, Phone: 608-262-5332, FAX: 608-262-3453, Email: record@biochem.wisc.edu.

binding and DNA wrapping by IHF in assembly of bacterial and phage multiprotein-DNA complexes *in vivo*; indeed this complex facilitates action-at-a-distance in transcription initiation, replication initiation, site-specific recombination, and transposition, and phage packaging [2; 3; 4; 5].

IHF heterodimers specifically recognize the H′ site (also the H1 and H2 sites) during λ phage integration into the *E. coli* chromosome.[6] Biophysical studies indicate that the bent and wrapped conformation of the H′ DNA observed in the co-crystal is adopted in solution. Lorenz et al used fluorescence resonance energy transfer (FRET) to determine the distance between fluorescent probes attached by six-carbon linkers at the ends of a 55 bp fragment with IHF bound at a central H′ site.[7] The observed interprobe distance (55 Å) is in close agreement with that predicted by projecting an additional helical turn (10 bp) from each end of the 34-mer in the cocrystal (52 Å)). Hydroxyl radical DNA footprinting studies indicate that the IHF – H′ DNA binding interface in solution is extensive, with protection extending over 30 bp.[8; 9] Formation of this interface at low [salt] is thermodynamically favorable at nM reactant concentrations.[7; 9; 10; 11; 12; 13] FRET-detected fast kinetic studies indicate that the mechanism of formation of the wrapped complex involves diffusion-limited initial binding followed by bending, with an activation energy for bending comparable to that for breathing of an AT base pair in a duplex.[14; 15]

DNA wrapping, the process whereby a protein binds and bends a large segment of DNA around its surface, is a common structural and mechanistic motif in large protein-DNA assemblies. In addition to the IHF – 34 bp H′ DNA complex, structurally well-characterized examples of wrapped DNA complexes include the nucleosome, with 147 bp of duplex DNA wrapped in 1.65 turns of a left-handed superhelix around the core histone octamer, and and the complex of E. coli single-stranded DNA binding protein (SSB) with two single-stranded dC_{35} oligomers, where the DNA is wrapped in a tennis ball seam pattern on the surface of SSB. Direct or indirect biophysical evidence has been obtained for DNA wrapping as part of the function of other nucleic acid binding proteins including RNA polymerase,[16; 17] UvrB,[18; 19] DNA gyrase,[20; 21; 22] topoisomerase IV,[23] lac repressor,[24] pepA,[25] and DnaA.[26] Investigations of the thermodynamics and mechanism of DNA wrapping have been conducted primarily with IHF [9; 27] and SSB.[15; 28; 29]

These three structurally-defined wrapped complexes all bury large numbers of DNA phosphates and cationic residues (primarily K, R: in some cases, H and/or the N-terminal amino groups) of the protein in the interface. Table 1 uses a 6 Å cutoff distance to characterize what groups are in proximity to one another in these wrapped interfaces. In the IHF – H′ DNA complex, 24 cationic groups and 4 anionic (D, E) groups are within 6 Å (see Table 1 and Fig 1) of an anionic phosphate oxygen of H′ DNA. (A complete distribution of charges in the vicinity of the interface is shown in Figure 1B). Strikingly, the composition of the IHF – H′ DNA interface (Figure 2) is very similar to that of the nucleosome, which is approximately 4 times larger, involves 5 times as many DNA phosphates and histone cationic groups, and bends DNA almost 4 times as much. In both complexes, almost 90% of protein-DNA contacts are with the DNA backbone.[30; 31] The SSB – ssDNA interaction involves stacking between DNA bases and aromatic protein residues, so is qualitatively distinct; the interface composition is accordingly similar but not identical to these wrapped interfaces involving ds DNA (see Figure 2 and Table 1).

In addition to its intrinsic interest and its value as a model system for the nucleosome and other large protein-nucleic acid assemblies, the IHF – H′ DNA interaction is an excellent system to investigate the contributions of salt ions and water of hydration to the thermodynamics of a protein-nucleic acid interaction. In particular, its large interface and numerous charge-charge appositions amplify the significance of coulombic, Hofmeister, and osmotic contributions.

Previous work in this area with IHF and SSB has demonstrated that, despite the large net positive charge on their DNA-binding surfaces, both systems exhibit DNA-binding constants which are much less [salt]-dependent than would be predicted by analogy to simple oligocation - DNA binding.[9; 27; 32; 33] DNA-binding of IHF and SSB is enthalpy-driven (highly exothermic) at 20°C, and this enthalpy is highly dependent on both [salt] and temperature.[27; 28; 32]

To gain a more detailed understanding of the driving forces and driven processes in DNA wrapping, we have quantified the always-large but anion-specific effects of KCl, KF, and KGlu on the binding constant, enthalpy, and entropy of specific binding of IHF to the H′ DNA site by isothermal titration calorimetry (ITC) and FRET. These data are interpreted using a novel thermodynamic analysis which separates coulombic, Hofmeister and osmotic effects of salt concentration, and predicts the amount and thermodynamic consequences of release of water and salt ions from the vicinity of the interfaces buried in complexation.

Results

FRET Determinations of IHF-H′ DNA Binding Constants (K_{obs}) as a Function of Concentration of Destabilizing Salts (KCl, KGlu) and a Stabilizing Osmolyte (Glyine Betaine)

IHF – H′ DNA binding analyzed by FRET provides both structural[7] and thermodynamic[14; 15] information. In a separate communication, the data are analyzed for structural information. Here the FRET assay is used to quantify and compare effects of [KCl] and [KGlu] on the binding constant K_{obs} for formation of the specific wrapped IHF – H′ DNA complex.

IHF Titrations at Constant Salt/Solute Concentration—Figure 3 shows the quality of representative data obtained in a forward FRET-detected titration of FAM-TAMRA labeled H′ DNA with IHF at 0.26 M KCl. As the IHF concentration is increased from 0 to 10 μM, emission spectra (counts/second) collected between 500 and 615 nm from solutions excited at 490 nm show a significant decrease in the FAM peak at 515 nm (Fig. 3A). Subtracting the emission spectrum from an intensity-normalized DNA fragment labeled only with FAM reveals the FRET effect as a concomitant increase in the TAMRA peak centered at 577 nm (Fig. 3B). Titrations of H′ DNA with IHF at constant salt concentration were analyzed by fitting theta (θ), the fractional increase in TAMRA emission, to a 1:1 binding model (see Methods).

The quality of FRET protein titrations and their fits are illustrated in Figure 4. Increasing [KCl] (Fig. 4A) or [KGlu] (Fig. 4B) weakens binding, as demonstrated by the increase in [IHF] required to attain half-saturation of the H′ site. Isotherms are well-fit by a single (1:1) binding mode at all [salt] investigated. The best fit value of the binding constant, K_{obs}, decreases from approximately $2.1 \times 108\ M^{-1}$ in 0.16 M KCl to 4.0×10^6 M in 0.26 M KCl (Table 2). In KGlu, K_{obs} decreases from $3.5 \times 107\ M^{-1}$ at 0.33 M to $1.5 \times 10^6\ M^{-1}$ at 0.68 M KGlu (Table 2). (Because binding is less [salt]-dependent in KGlu than in KCl, a wider and higher range of [KGlu] could be investigated.) Plots of log K_{obs} from FRET experiments vs log $[K^+]$ are linear within the uncertainty (see Fig. 8 below); the slopes $SK_{obs} \equiv d\ln K_{obs}/d\ln[K^+]$ differ by a factor of two (approximately −9.1 in KCl and −4.6 in KGlu; Table 3).

Salt/Solute titrations of IHF/H′ DNA Mixtures—To examine in more detail the roles of salt ions and water on the thermodynamics of forming IHF – H′ DNA complexes, mixtures of IHF and H′ DNA were titrated with KCl, KGlu or glycine betaine (GB) and assayed by FRET. These experiments allow a direct measurement of the effect of [solute] on the equilibrium extent of binding. In a “salt-back” titration, a solution of IHF – H′ DNA complexes (1:1 ratio of IHF to H′DNA) initially at 0.182 M K^+ (i.e. 0.16 M X^-) was titrated with KCl or KGlu. Titration with either salt drives dissociation of IHF – H′DNA complexes, resulting in an increase in FAM donor emission and a corresponding decrease in TAMRA emission. A

representative FRET-detected salt-back titration with KGlu is shown in Figure 5A. As [KGlu] is increased from 0.16 M to 0.72 M, the TAMRA emission decreases by > 90%. Analysis of these data (see Methods and Supplemental Fig 1) reveals that the fraction of H′ DNA complexed with IHF (θ) decreases from saturation to zero over this range of [KGlu]. The resulting log K_{obs} values (determined from data in which $0.1 < \theta < 0.9$) are plotted as a function of log $[K^+]$ in the inset to Fig. 5A, yielding $SK_{obs} = -5.1$ for this representative titration. Values of SK_{obs} determined by FRET salt-back titrations agree well with those determined by protein titrations (see Table 3). These large differences in K_{obs} and in SK_{obs} for K^+ salts of Cl^- and Glu^- demonstrate that one or both of these salt anions is/are exerting more than a purely coulombic effect on the binding free energy.

In contrast to the destabilizing effects of salt, the osmolyte GB stabilizes protein-nucleic acid complexes. Because GB is strongly excluded from the water of hydration of anionic surface and does not appear to be either excluded or accumulated to a significant extent from other types of surface of most globular proteins and duplex DNA,[34; 35] this osmolyte drives binding of IHF to H′ DNA and other processes which bury and dehydrate anionic surface (in this case primarily anionic DNA phosphate oxygens). Analysis of thermodynamic data for the interaction of GB with anionic surfaces of proteins and DNA indicates that the hydration of this surface is approximately 0.22 H_2O per Å^2.[34; 35] In the IHF – H′ DNA crystal structure, 1200 Å^2 of anionic surface are buried (almost entirely DNA phosphate oxygens). If this surface dehydrates significantly in complexation, the stability ($\Delta G°_{obs} = -RT\ln K_{obs}$) of the IHF-H′ DNA complex is predicted to increase approximately linearly with [GB], and the initial slope of this plot (the GB *m*-value) provides a measure of the net amount of water released from anionic surface in complex formation.[36; 37]

To apply this analysis, 1:1 mixtures of IHF and H′ DNA at a FRET-detectable DNA concentration and a salt concentration at which the extent of binding is initially small (initial $\theta < 0.3$ in the absence of GB) were titrated with glycine betaine. A representative titration (monitored by TAMRA emission) is shown in Figure 5B. Addition of GB drives binding, causing the TAMRA emission to increase by > 100%. Analysis of these data (see Methods and Supplemental Fig 1) shows that θ increases from 0.29 (in the absence of GB) to 0.87 (at 1.5 M GB) and that K_{obs} for IHF-H′DNA binding increases by more than an order of magnitude per molar GB added. For [GB] < 1.5 M, a semi-log plot of K_{obs} as a function of [GB] is linear (see inset to Fig. 5B), and yields a slope $d\ln K_{obs}/d[GB] = 2.9 \pm 0.4$. Due to the favorable preferential interaction of GB and KCl, a small correction is necessary, yielding $d\ln K_{obs}/d[GB] = 2.7 \pm 0.4$ at constant KCl activity (see Methods). Above 1.5 M GB, preliminary data indicate that K_{obs} attains a broad maximum and then decreases at high [GB]. Similar effects of high [GB] have been previously observed on K_{obs} for protein folding and for binding of lac repressor to lac operator DNA.[37; 38; 39]

ITC determinations of $\Delta H°_{obs}$ and K_{obs} for IHF-H′ DNA Interactions from Forward and Reverse Titrations

Binding Enthalpies $\Delta H°_{obs}$—ITC detects the heat absorbed or evolved for each sequential addition of one reactant to the other, providing a direct measure of the enthalpy change $\Delta H°_{obs}$ for formation of the IHF-H′ DNA complex. Figure 6 plots enthalpy data for forward (IHF into H′ DNA) and reverse (H′ DNA into IHF) ITC titrations at representative concentrations of KCl (panels A, B), KF (panel C) and KGlu (panel D). Other examples of ITC data and baseline controls for forward and reverse titrations at high and low concentrations of the salts investigated are shown in Supplemental Figures 2 and 3. In KCl, the binding enthalpy (observable in Fig. 6 as the plateau at the beginning of each titration where there is complete binding of all the titrant added) increases strongly (i.e. decreases in magnitude) with increasing salt concentration. In contrast, $\Delta H°_{obs}$ increases modestly with increasing [KGlu] or [KF].

These dependences of the binding enthalpy on salt concentration for the three K^+ salts investigated (KCl, KF, KGlu) are shown in Figure 7. In all cases, binding is exothermic at 20° C with enthalpies ranging from approximately −20 kcal · mol^{-1} at 0.04 M KCl or KF to −5 kcal · mol^{-1} at 0.53 M Glu^-. Binding enthalpies increase linearly with salt molarity in all three salts. In the low salt limit ($[K^+] \rightarrow 0$), $\Delta H°_{obs}$ approaches −21 kcal · mol^{-1} in KCl and KF, and −10 kcal · mol^{-1} in KGlu. Although the binding enthalpies in KGlu increase in parallel with those in KF, they are systematically offset by 11 kcal · mol^{-1} (Figure 7). We interpret this offset as the result of uptake of 1.1 ± 0.2 protons by IHF in binding H′ DNA (data not shown) because the enthalpies of deprotonation of glutamate and phosphate differ by 10 kcal · mol^{-1} (see Supplemental Text). The slope $d\Delta H°_{obs}/d[K^+]$ is much larger in KCl than in KF or KGlu (8.5 ± 0.8); see Discussion. For all three salts investigated, the [salt]-dependence of the enthalpy is much larger than that expected for a purely coulombic salt effect, which should be primarily entropic in water.[40; 41; 42; 43]

Binding Constant K_{obs}—For the high-purity oligomer strands investigated here, under solution conditions where the binding constant K_{obs} does not exceed 3×10^7 M^{-1}, fits to the ITC enthalpy data as a function of titrant concentration (Figure 6) are expected to provide accurate determinations of K_{obs} for binding of IHF to the intact 34 bp duplex. For all three salts investigated, binding constants decrease with increasing salt concentration, as evidenced in Figure 6 by an increase in breadth of the late sigmoid region of the enthalpy-monitored binding isotherms (the region where a significant fraction of the titrant is unbound). Thermodynamic quantities obtained from the ITC data of Figure 6 are listed in Table 4. As observed above using FRET, binding is detectably tighter in Glu^- (and F^-) relative to Cl^-. For all salt concentrations examined, binding is enthalpically driven and opposed by the entropic contribution to $\Delta G°_{obs}$.

Comparison of FRET and ITC-Determined Binding Constants as a Function of [KX]

Values of K_{obs} determined by FRET and ITC experiments (Tables 2 and 4, respectively) as a function of [KX] are directly compared on a log-log scale in Figure 8. At the same [KX], K_{obs} determined by FRET are uniformly larger than those determined by ITC. We hypothesize that the one base overhang and/or the fluorophores present in FRET studies contribute favorably to binding (see Supplemental Text), consistent with the observation that the TAMRA quantum yield increases by ca. 20% in the complex relative to its value in free DNA (data not shown). Favorable interactions with fluorophores are also exhibited by SSB where a 10-fold increase in binding strength together with an increase in the quantum yield for Cy3 was found for a FRET-labeled $(dT)_{70}$ construct.44 In our FRET studies at 20°C, performed at free [IHF] ranging from 1 nM to 10 μM, IHF dimer dissociation does not make a detectable contribution to the binding assay (see Supplemental Text).

Although values of SK_{obs} for the different H′ DNA fragments investigated by FRET and ITC in principle will differ because of the greater number of negative charges (a total of 6 more negative charges) at the ends of the FRET fragment, no significant difference was detected in fits to the individual datasets (Table 3). To combine the two data sets and obtain the best fit SK_{obs}, a constant offset was applied to values of log K_{obs} for the FRET fragment (0.6 in KCl, 0.9 in KGlu; see Supplemental Text). The combined data together with the combined ITC enthalpies are reported and analyzed in Figure 9 below.

Discussion

Salt concentration, cation valence and the chemical identity of the salt anion are key determinants of stability ($\Delta G°_{obs}$) of virtually all protein-nucleic acid complexes. Well-studied examples include the interactions of *E. coli* lac repressor tetramer with operator and

nonoperator DNA and of *E. coli* RNA polymerase with promoter and nonpromoter DNA (see for example: [45; 46; 47; 48]). At constant [salt] (0.13 M), the lac repressor – lac operator binding constant increases by a factor of 10^4 as the anion is varied across the Hofmeister series from I^- to F^-.[46] Analogous effects are observed on the thermodynamics of interactions of single-strand binding proteins with single-stranded DNA (see for example: [33; 49]). Generally, for any choice of anion, K_{obs} decreases strongly with increasing [salt]. In Cl^- salts (KCl or NaCl), in the absence of Mg^{2+} divalent cations, values of SK_{obs}, the log-log derivative of the binding constant with respect to [salt], range from −5 to −11 for various specific and nonspecific lac repressor–DNA complexes,[45] and from −8 to −20 for various RNA polymerase – DNA complexes.[47; 50] for *E. coli* SSB, a detailed series of studies by Kozlov and Lohman have characterized the large effects of salt concentration and the nature of the anion on $\Delta H°_{obs}$ and, where accessible, K_{obs} of complex formation.[28; 32; 33] The extensive set of data reported here quantifying the large effects of [KCl], [KF] and [KGlu] on K_{obs} and $\Delta H°_{obs}$ for the large-interface specific complex between IHF and H′ DNA (summarized in Figure 9) provide an opportunity to develop and test a general quantitative interpretation of coulombic, Hofmeister and osmotic effects of salt concentration on protein-nucleic acid interactions. While K_{obs} is expected to exhibit a strong dependence on [salt] (at low [salt]) because of the neutralization of DNA phosphate charge by basic protein side chains in the interface, this coulombic effect is not expected to be anion-specific. Moreover, since coulombic effects of [salt] are primarily entropic in aqueous solution, they are not the origin of the effects of [salt] on $\Delta H°_{obs}$.

Both K_{obs} and $\Delta H°_{obs}$ for the specific wrapping of duplex DNA on IHF are much more [salt]-dependent in KCl than in KF or KGlu, whose effects are indistinguishable within uncertainty. For the combined ITC/FRET data sets, Panel A of Figure 9 shows that SK_{obs} is approximately twice as large in magnitude in KCl (−8.8 ± 0.7) as in the combined KF/KGlu dataset (−4.7 ± 0.6). At an intermediate [salt] (0.33 M) where only minimal extrapolation is needed to compare the Cl^- and the combined F^-/Glu^- data sets, K_{obs} is approximately 30-fold larger in KF/KGlu than in KCl (Table 3). Determinations of the binding enthalpy $\Delta H°_{obs}$ extend to lower [salt] (0.06 M salt) where K_{obs} is too large to measure by either assay. For each salt investigated, corrected values of $\Delta H°_{obs}$ decrease linearly with decreasing [salt] and approach the same limiting low-salt value ($\Delta H°_{obs}$ = −20 kcal at 20°C) for all three salts studied (Figure 9B). The slope ($d\Delta H°_{obs}/d[salt]$) is much larger in KCl (38 ± 3) than in the combined KF/KGlu dataset (11 ± 2).

Dissecting the [Salt]-Dependences of K_{obs} and $\Delta H°_{obs}$ into Coulombic and Hofmeister-Osmotic Contributions

To interpret these strong and anion-specific effects of [salt] on K_{obs} and $\Delta H°_{obs}$ of binding of IHF to H′DNA, we develop and apply a novel analysis which dissects the experimental SK_{obs} and the derivative $d\Delta H°_{obs}/d[salt]$ into a) Coulombic and b) Hofmeister-osmotic contributions.

a) Coulombic contributions—Coulombic contributions of [salt] are defined as those arising from differences in long-range (coulombic) interactions of salt ions with structural charges on the IHF – H′ DNA complex and on the uncomplexed IHF and H′DNA. Since coulombic effects depend on the valence of the salt ion but not its chemical identity, they should be the same for all three 1-1 salts investigated. Coulombic effects on processes involving nucleic acids are manifested even at very low salt concentration.[51; 52] for IHF – H′ DNA binding, coulombic effects are expected to be the primary salt effect at low [salt], since no evidence exists for strong site-binding of any of these salt ions to IHF or duplex DNA. For binding of an oligocation L^{Z+} to a polyanionic nucleic acid at low salt concentration, where salt effects appear to be purely coulombic,[40; 41; 53; 54; 55] the observed log-log derivative of the binding constant with respect to salt concentration

$SK_{obs} = d\ln K_{obs}/d\ln[salt] = SK_{obs}^{coulombic}$ is negative, relatively independent of [salt] and temperature, and proportional to the oligocation valence Z. The strong increase in K_{obs} for DNA-binding of L^{Z+} with decreasing salt concentration is an entropic effect, as expected for a process that reduces local salt ion concentration gradients. By analogy to PB calculations for other protein-nucleic acid interactions, $SK_{obs}^{coulombic}$ for binding IHF to H′DNA is also expected to be relatively independent of [salt] and temperature.[56; 57; 58; 59; 60]

b) Hofmeister-osmotic contributions—At moderate to high concentrations, salts affect processes like the creation of an air-water interface and the transfer of a hydrocarbon solute to water in which only uncharged surfaces are involved and no coulombic effect is expected. These salt effects exhibit a distinct functional form, in which $\Delta G°_{obs}$ of the process is typically a linear function of [salt]. Both the functional form and rank order of these salt effects on model processes mirror what are referred to as Hofmeister effects of salts at moderate to high concentrations on biopolymer processes involving changes in ASA (e.g. unfolding, dissociating or dissolving biopolymers).[61; 62] The solute partitioning model [34; 38; 63; 64; 65; 66; 67] (SPM) dissects these salt effects into an ion-specific competition with hydration water to make short-range (noncoulombic) interactions with the biopolymer surface (described by partition coefficients K_p for cation and anion) and a nonspecific (osmotic) component arising from the reduction in water activity with increasing salt concentration, which drives processes in the direction in which hydration water is released. The SPM has recently been applied to interpret effects of salts on the surface tension of water and obtain individual partition coefficients of the cation and anion describing their distributions between local water at the air-water interface and bulk water.[65; 66]

Here we use the term Hofmeister effect to refer only to the ion-specific (nonosmotic) part of this composite salt effect. In the following thermodynamic analysis, the SPM is introduced to quantify and interpret the contributions of Hofmeister and osmotic effects to the [salt]-dependences of K_{obs} and $\Delta H°_{obs}$ of biopolymer processes like IHF – H′ DNA binding.

Thermodynamic Analysis of Coulombic and Hofmeister-Osmotic Contributions to the [Salt] Dependences of K_{obs} and $\Delta H°_{obs}$; Comparison with the Effect of a Nonelectrolyte

To interpret salt effects on K_{obs}, we begin by assuming that SK_{obs}, the log-log salt derivative of K_{obs}, is composed of additive contributions from coulombic effects $SK_{obs}^{coulombic}$ and Hofmeister-osmotic effects $SK_{obs}^{Hof-osm}$ of salt concentration,[52] as defined above:

$$\frac{\partial \ln K_{obs}}{\partial \ln[KX]} \equiv SK_{obs} = SK_{obs}^{coulombic} + SK_{obs}^{Hof-osm} \quad (2)$$

To test the validity of the assumption of additivity of coulombic and Hofmeister-osmotic effects, which is the only currently feasible starting point for this analysis, it will be important to quantify the noncoulombic (i.e. Hofmeister) component of the interactions of salt ions with compounds that model the charged, polar and nonpolar sub-surfaces of proteins and nucleic acids. We also assume that $SK_{obs}^{coulombic}$ is independent of temperature (because coulombic salt effects in water are largely entropic) and [salt], and is the same for all 1-1 salts. For binding of oligolysines and polyamines to DNA, which appear to be primarily coulombic interactions, SK_{obs} is indeed independent of salt concentration in the accessible range (below 1 M salt), independent of temperature and the same for the various small 1:1 salts investigated.[68; 69]

The solute partitioning model (SPM) predicts that $SK_{obs}^{Hof-osm}$ is proportional to [salt], with a proportionality constant which is determined by a) the amount of water of IHF and DNA hydration which is displaced/released in forming the complex (ΔB_{H_2O}) and b) the partition

coefficients $K_{p,i}$ of the cation and anion which describe the ratio of their local concentrations in *this* water of hydration to their bulk concentration. The difference in the amount of water of hydration of the product complex and the uncomplexed reactants is defined as ΔB_{H_2O}; $\Delta B_{H_2O} = b_{H_2O}\,\Delta\mathrm{ASA}$, where ΔASA is the difference in water accessible surface area (ASA) between the IHF – H′ DNA complex and the uncomplexed reactants, and b_{H_2O} is the average hydration of those reactant 2 surfaces which are buried in the interface in the complex.

$$SK_{obs}^{Hof-osm} = (K_{p+} + K_{p-} - 2)\frac{\Delta B_{H_2O}}{m^{\bullet}_{H_2O}}(1 + \delta_{KX})[KX] \tag{3}$$

where $m^{\bullet}_{H_2O} = 55.5$ mol H_2O/kg, δ_{KX} is a relatively small correction term ($|\delta_{KX}| \ll 1$) for salt nonideality and concentration scale conversion, and the ion partition coefficients $K_{p,i}$ are defined as:

$$K_{p,K^+} = \left(\frac{m^{loc}_{K^+}}{m^{bulk}_{K^+}}\right) \quad \text{and} \quad K_{p,X^-} = \left(\frac{m^{loc}_{X^-}}{m^{bulk}_{X^-}}\right) \tag{4}$$

For formation of the wrapped IHF – H′ DNA complex, ΔB_{H_2O} is expected to be large and negative; from the estimated ΔASA of complexation (−5340 Å^2) and the model compound estimate of b_{H_2O} (0.18 H_2O/Å2), $\Delta B_{H_2O} = -10^3$ H_2O.

The SPM also predicts the dependence of K_{obs} of IHF-H′ DNA binding (or any other process) on the concentration of a nonelectrolyte like glycine betaine:

$$\frac{\partial \ln K_{obs}}{\partial [GB]} = (K_{p,GB} - 1)\left(\frac{\Delta B_{H_2O}}{55.5}\right)(1 + \delta_{GB}) \tag{5}$$

In equation 5, δ_{GB} is a correction term ($|\delta_{GB}| \ll 1$) for GB nonideality and concentration scale conversion. For glycine betaine, the composite term ($K_p - 1$) ΔB_{H_2O} in Eq 5 has been dissected into contributions from different types of biopolymer surface. At a coarse-grained level, glycine betaine is found to be completely excluded ($K_{p,GB}^{anionic} = 0$) from approximately two layers of water of hydration (0.22 H_2O/Å^2) of anionic surface, but not significantly excluded from (or accumulated at) other types (nonpolar, polar, cationic) of protein or native dsDNA surface ($K_{p,GB}^{nonanionic} = 1$). However, GB accumulates near guanidine and/or cytosine rings, which complicating its effect on ssDNA processes. A similar decomposition for Hofmeister salts is in progress. for GB, therefore, eq. 5 becomes

$$\frac{\partial \ln K_{obs}}{\partial [GB]} = -0.018\Delta B_{H_2O}^{anionic\ surface} \quad (for\ [GB] \to 0) \tag{5A}$$

and the dependence of ln K_{obs} of IHF-H′ DNA binding on [GB] is predicted to provide a direct measure of the amount of water released from anionic (primarily DNA phosphate, possibly also IHF carboxylate) surface in complex formation.

For salts, integration of Eqs. (1, 2), neglecting any concentration-dependence of δ, yields Eq. 6 for K_{obs} as a function of concentration of any salt, relative to its extrapolated value at a sufficiently low reference salt concentration (K_{ref}) where only coulombic effects of salt are significant.

$$\log K_{obs} = \log K_{ref} + SK_{obs,coul}\log\left(\frac{[KX]}{[KX]_{ref}}\right) + 1/2.303\left(\frac{\Delta B_{H_2O}}{m^{\bullet}_{H_2O}}\right)(K_{p,K^+} + K_{p,X^-} - 2)([KX] - [KX]_{ref})(1 + \delta_{KX}) \tag{6}$$

Differentiation of Eq. 3 with respect to temperature yields Eq. 7 for the [salt]-derivative of the binding enthalpy:

$$\frac{\partial \Delta H^{\circ}_{obs}}{\partial [KX]} = RT^2 \frac{\partial}{\partial T} \frac{\partial \ln K_{obs}}{\partial [KX]} = \frac{\Delta B_{H_2O}}{m^{\bullet}_{H_2O}} (K_{p,K^+} \Delta H^{\circ}{}_{p,K^+} + K_{p,X^-} \Delta H^{\circ}{}_{p,X^-})(1 + \delta_{KX}) \quad (7)$$

where $\Delta H^{\circ}{}_{p+}$ and $\Delta H^{\circ}{}_{p-}$ are the van't Hoff enthalpy changes for the process of transferring cations and anions from bulk solution to the relevant water of hydration of IHF and H′DNA ($\Delta H^{\circ}{}_{p+} = RT^2 d\ln K_{p+}/dT$).

The net effect of the opposing contributions of Hofmeister interactions and osmotic effects of salt ions on the observed salt derivative SK_{obs} (eq. 2) and therefore on log K_{obs} (eq. 6) for a 1:1 salt is determined by the quantity ΔB_{H_2O} ($K_{p+} + K_{p-} - 2$). For the nonelectrolyte glycine betaine, the analogous term in eq. 5 is ΔB_{H_2O} ($K_{p,GB} - 1$). The integer (−2 for a 1:1 salt, −1 for a nonelectrolyte) is the purely osmotic contribution of the solute (a driving force for complexation with increasing [solute] because of displacement/release of water of hydration). [70; 71; 72; 73] for 1:1 salts this purely osmotic effect is reduced (and can be eliminated or reversed) if either or both salt ions compete with water of hydration (i.e. $K_{p,i} > 0$) to interact noncoulombically with the surfaces of IHF and H′ DNA which are buried and desolvated in the complex. For a 1:1 salt, osmotic and Hofmeister effects completely compensate if $K_{p+} + K_{p-} = 2$, in which case the average local concentration of salt ions (cation plus anion) in the vicinity of the reactant IHF and H′ DNA surfaces which are buried in complexation is equal to the bulk concentration of salt ions. In this case Hofmeister and osmotic contributions to SK_{obs} sum to zero. For salts where $K_{p+} + K_{p-} > 2$, Hofmeister interactions of the ions with the relevant biopolymer surfaces are dominant over the osmotic effect, and the combined Hofmeister-osmotic contribution destabilizes complexes with increasing [salt].

Since osmotic and coulombic effects of salts on processes in water are primarily entropic, only the Hofmeister interaction of salt ions with biopolymer surfaces (quantified by $K_{p,i}$) contributes to the salt dependence of the binding enthalpy. Eq. 7 shows that the derivative $d\Delta H^{\circ}_{obs}/d[salt]$ is determined by the product ΔB_{H_2O} ($K_{p+}\Delta H^{\circ}{}_{p+} + K_{p-}\Delta H^{\circ}{}_{p-}$). Hence ΔH°_{obs} of IHF-H′ DNA binding (or any other process) is predicted to be independent of [salt] for a completely excluded salt. For salts which are not completely excluded and for which the enthalpies of transfer of salt ions from bulk solution to the relevant regions of biopolymer surface are negative, the binding enthalpy ΔH°_{obs} is predicted to increase with increasing [salt] (since $\Delta B_{H_2O} < 0$). For a salt in the middle of the Hofmeister series ($K_{p+} + K_{p-} = 2$), the [salt] dependence of the binding constant is predicted to be equal to the coulombic contribution ($SK_{obs} = SK^{coulombic}_{obs}$) because $SK^{Hof-osm}_{obs} = 0$, while the [salt] dependence of the binding enthalpy ($d\Delta H^{\circ}_{obs}/d[salt]$) can be much greater than the negligible small coulombic contributions if Hofmeister interactions have significant enthalpies ($\Delta H^{\circ}{}_{p+}$, $\Delta H^{\circ}{}_{p-}$).

Application to Effects of Salts (KCl, KF, KGlu) and Glycine Betaine on the Thermodynamics of IHF-H′ DNA Binding

a) Salt Effects—KCl is typically in the middle of the Hofmeister series; changes in [KCl] in the molar range typically have only small effects on protein processes, relative to salts from the extremes of the Hofmeister series. For purposes of illustration, and as a first order approximation to the likely behavior of IHF – H′ DNA binding, we assume that $K_{p,K+} = K_{p,Cl-} = 1$ so that $SK^{Hof-osm}_{obs,KCl} = 0$ and $SK_{obs,KCl} = SK^{coulombic}_{obs(1:1salt)} = -8.8$. This is a large coulombic effect, but it is much smaller in magnitude than that predicted by analogy to oligocation binding ($SK_{obs} = -18$) using the net cationic charge on the interface of IHF (+20).

To interpret the shifts in K_{obs} and in SK_{obs} in the combined KF/KGlu data set relative to KCl requires knowledge of ΔB_{H_2O}. No direct measurement of this quantity is available, but its value can be estimated from the application of the SPM to interpret salt effects on the solubility of model compounds, for which ΔB_{H_2O} = 0.18 $H_2O/Å^2$ (LM Pegram, unpublished results). Similar values have been obtained from the SPM for the thickness of the local region at the air-water interface (0.19 $H_2O/Å^2$)66 and for the hydration of anionic biopolymer surface (0.22 $H_2O/Å^2$).38 From the estimated ΔASA of formation of the IHF – H′ DNA complex (−5340 $Å^2$) and the model compound estimate of b_{H_2O} (0.18 $H_2O/Å^2$), ΔB_{H_2O}= −1000 H_2O. Fixing the values of ΔB_{H_2O}, $SK^{coulombic}_{obs(1:1salt)}$, $K_{p,K+}$, and $K_{p,Cl-}$ to the above best estimates, the combined KF/KGlu data set (log K_{obs} vs. log $[K^+]$) was fit to Eq. 6. The resulting fitted curve yields $K_{p,F-} = K_{p,Glu-}$ = 0.44, so that moderate exclusion of F^- and Glu^- is capable of describing the shift in both K_{obs} and SK_{obs} in KF/KGlu relative to KCl. The curvature predicted by the fit is consistent with these KF/KGlu binding data, though they could be equally well fit by a straight line. The curve shown for the combined KF/KGlu dataset in Fig 9 uses the KF activity coefficient and molarity conversion term ($1 + \delta_{KF}$). Slightly more curvature is predicted in the plot of log K_{obs} for this parameter set using the conversion for KGlu; we are currently testing for the presence of this curvature at higher [KF] or [KGlu].

The parameters used in Figure 9 (ΔB_{H_2O}= −1000 H_2O, $K_{p,K+} = K_{p,Cl-}$ = 1, $K_{p,F-} = K_{p,Glu-}$ = 0.44) are a plausible set of SPM quantities to describe salt effects on log K_{obs} for IHF – H′ DNA binding. Are these capable of describing the experimental salt effects on $\Delta H°_{obs}$? From Figure 9B we see that the answer is in the affirmative; the linear increases in $\Delta H°_{obs}$ with increasing salt concentration, with a slope $d\Delta H°_{obs}/d[salt]$ in KCl which is significantly larger than in KF/KGlu, are clearly consistent with equation 7 and with partition coefficients of K^+ and Cl^- which are larger than those of F^- and Glu^-, provided that the local-bulk partitioning enthalpies of these salts are negative and of similar magnitudes. At a more quantitative level, it is clear that the almost four-fold difference in slopes $d\Delta H°_{obs}/d[salt]$ between them is much greater than the approximately two-fold difference in anion partition coefficients. If all the ion partitioning enthalpies are small in magnitude, which is consistent with data on the temperature dependences of $d\Delta H°_{obs}/d[salt]$ (Vander Meulen PhD thesis, 2007), it is necessary that the partitioning enthalpies of both K^+ and Cl^- be negative, and that the partitioning enthalpy of Cl^- be significantly more negative than that of F^- or Glu^-. With two equations and three unknowns, the values of individual ion partition coefficients cannot be uniquely determined. A typical set is used to obtain the fits in Figure 9B: $\Delta H°_{p,K+}$ = −1.3 kcal, $\Delta H°_{p,Cl-}$ = −1.0 kcal, $\Delta H°_{p,F-} = \Delta H°_{p,Glu-}$ = +1.6 kcal. The composite set of SPM salt ion parameters used in Figure 9 is listed in Table 5.

b) Effect of GB—Since the primary interaction of GB with native protein and DNA surface is complete exclusion from two layers of water of hydration of anionic surface, the effect of GB on the IHF-DNA binding constant quantifies the net amount of water of hydration of anionic surface released in forming the complex. From the structure, approximately 1200 $Å^2$ of DNA phosphate surface are buried in the complex, and therefore approximately 260 H_2O would be released from DNA phosphates if they were completely dehydrated in the complex (ΔB_{H_2O}= −260). The derivative of ln K_{obs} with respect to [GB] at constant KCl activity, $d\ln K_{obs}/d[GB])_{aKCl}$ = 2.7 ± 0.4, indicates that about half that number of H_2O are released (ΔB_{H_2O}= −150). This might mean that about half of the original amount of water of DNA phosphate hydration is retained in the interface. Alternatively, or additionally, a significant amount of water might be taken up by anionic surface exposed in a process coupled to DNA binding, as for example if salt bridges between carboxylate and basic side chains of IHF break and hydrate in complexation.[27]

Thermodynamics of IHF-H′DNA Binding: Prediction of High and Low Salt Behaviors of $\Delta G°_{obs}$, $\Delta H°_{obs}$, and $T\Delta S°_{obs}$ in KCl and KF or KGlu

In the range of salt concentrations investigated (> 0.15 M for K_{obs}, > 0.06 M for $\Delta H°_{obs}$), predicted Hofmeister and osmotic contributions to K_{obs} and Hofmeister contributions to $\Delta H°_{obs}$ of formation of this large interface protein-DNA specific complex are always significant. Figure 10 predicts the effects of lower and high salt concentrations, based on Eqs 6 and 7, and predicts the decomposition of $\Delta G°_{obs} = -RTln(K_{obs})$ into enthalpic ($\Delta H°_{obs}$) and entropic ($T\Delta S°_{obs}$) contributions over this wide [salt] range in both KCl and KF/KGlu. Because $\Delta H°_{obs}$ and the Hofmeister and osmotic contributions to $\Delta G°_{obs}$ and $T\Delta S°_{obs}$ vary linearly with [salt] whereas the coulombic contribution to $\Delta G°_{obs}$ and $T\Delta S°_{obs}$ varies linearly with the logarithm of [salt], plots of these thermodynamic quantities vs. both [salt] and log [salt] are informative. For KCl and KF/KGlu, Figure 10A shows the predicted nonspecific osmotic contribution and salt-specific Hofmeister contributions to $\Delta G°_{obs}$, $\Delta H°_{obs}$ and $T\Delta S°_{obs}$ as functions of salt concentration (linear scale, the appropriate functional form for these effects). Figures 10B and 10C extrapolate the observed $\Delta G°_{obs}$, $\Delta H°_{obs}$ and $T\Delta S°_{obs}$ of IHF – H′ DNA binding to low and high concentrations of these salts (0.005 M – 2 M), using a log [salt] scale on which coulombic effects are linear.

At sufficiently low salt concentration (< 0.05 M), Hofmeister and osmotic effects do not contribute significantly to $\Delta G°_{obs}$, $\Delta H°_{obs}$ and $T\Delta S°_{obs}$ of IHF-H′DNA binding in any 1:1 salt, and all these thermodynamic quantities are predicted to be the same for any 1:1 salt. In this low salt regime, $\Delta G°_{obs}$ and $T\Delta S°_{obs}$ are predicted to vary linearly with log [salt] because the origin of the [salt] dependence is entirely coulombic, and $\Delta H°_{obs}$ is predicted to be essentially independent of [salt]. Different PNAI, with different ΔB_{H_2O}, will exhibit correspondingly different cutoffs for the low-salt all-coulombic regime of [salt] effects. At higher salt concentrations, differences in $\Delta H°_{obs}$ for different salts and different [salt] become detectable, and $\Delta G°_{obs}$ and $T\Delta S°_{obs}$ in general deviate from the low-salt all-coulombic [salt] dependence.

For KCl, in the scenario modeled here, $\Delta G°_{obs}$ does not deviate from a coulombic salt dependence because of the postulated compensation between Hofmeister and osmotic contributions of this salt to SK_{obs}. $T\Delta S°_{obs}$ does deviate from a coulombic dependence because this compensation does not apply at the level of $T\Delta S°_{obs}$ (equations 6 and 7). At salt concentrations higher than the experimental range (experimentally inaccessible), a regime of approximate enthalpy-entropy compensation is predicted, in which $\Delta H°_{obs}$ and $T\Delta S°_{obs}$ vary much more strongly with KCl concentration than does $\Delta G°_{obs}$. (This compensation will be even more complete at the level of $\Delta G°_{obs}$ if the coulombic component of SK_{obs} is reduced in magnitude at high salt concentration.)

For KF/KGlu, $\Delta G°_{obs}$ and $T\Delta S°_{obs}$ begin to deviate significantly from the universal purely-coulombic behavior predicted for any 1:1 salt at approximately 0.05 M KF/KGlu because the osmotic contributions of these salts with excluded anions to SKobs exceed their Hofmeister contributions. As a result, above 0.05 M salt, K_{obs} of IHF – H′ DNA binding is larger in KF/KGlu than in KCl. The thermodynamic origin of this effect is the more favorable $\Delta H°_{obs}$ in KCl; the molecular origin is the stronger interaction of Cl^- than of F^- or Glu^- with the surfaces of free IHF and H′ DNA that are buried in the interface of the complex. Formation of the complex displaces/releases salt ions and water; the salt ion contribution arises from changes in both coulombic and Hofmeister interactions in complexation. For KCl, the thermodynamic contribution of displacing ions and water is the same at all [salt]; for KF/KGlu this contribution becomes increasingly favorable with increasing [salt] because the replacement of Cl^- ($K_p = 1$) with F^- or Glu^- ($K_p = 0.4$) causes the osmotic effect of increased [salt] to exceed the Hofmeister interaction effect. At salt concentrations only slightly above the experimental range, $\Delta G°_{obs}$ is predicted to exhibit a local maximum, and then decrease at higher [salt]. In this same range of

[salt], enthalpy-entropy compensation is predicted for KF/KGlu, as for KCl; $\Delta H°_{obs}$ and $T\Delta S°_{obs}$ are predicted to vary much more strongly with [salt] than does $\Delta G°_{obs}$.

Methods

IHF

IHF was overexpressed from a pET21a vector (a gift from Phoebe Rice) in a 60 L fermenter, and purified in 200 g frozen cell paste increments. Purification followed the scheme of Nash et al.[74] with slight modifications as decribed previously.[27] IHF was determined to be > 95% pure by SDS-PAGE; the concentration was determined using an extinction coefficient (280 nm) of 4920 M^{-1} cm^{-1}.[27] Circular Dichroism (CD) and Differential Scanning Calorimetry (DSC) were used to show that, at μM concentrations required for ITC, the folded αβ dimer of IHF is stable at 20°C at both 0.04 M and 0.20 M KCl. Likewise, ITC dilution experiments with IHF and FRET binding assays show no evidence for dissociation of the IHF dimer at 20°C.

In ITC experiments, the DNA binding activity of IHF, as determined from the titration stoichiometry, was routinely ≥90%. In FRET experiments, however, IHF adsorption to eppendorf vials during sample preparation reduced the effective protein activity. FRET activity measurements (below) were carried out in parallel with binding constant assays. The activity assay was performed by titrating 35 nM H′ DNA with the highest concentration IHF stock solution used for the binding assay (ca. 1 μM IHF; see FRET sample preparation details below). The buffer was diluted with a low salt buffer such that the final [KCl] was 0.13 M or [KGlu] was 0.18 M. Binding under these conditions is essentially stoichiometric to 80% saturation of the DNA, and the curve in this region was extrapolated to the signal plateau to determine the binding activity. By this method, the activity of a nominal 1 μM stock IHF preparation was routinely 75% –100%.

In FRET binding assays, data points at low [IHF] were collected using IHF from a lower concentration (ca. 0.2 μM) IHF stock solution, which displayed a further reduction in effective IHF activity. The activity of this stock was determined by performing duplicate measurements at various IHF concentrations, using both the high and low concentration IHF stock solutions, and attributing the difference in the FRET signal to protein activity. The activity was routinely ca. 50% for the low concentration stock solutions. The simplicity of this activity correction is warranted, based on IHF dimer stability measurements (cited above) and control experiments (below) that eliminated possible complications from time- or concentration-dependent dissociation of IHF dimers at 20°C.

DNA oligomers

The H′ DNA site is a GC-capped 34 bp duplex matching the λ phage H′ site, with the same sequence but lacking the 5′ overhanging bases and nick(s) of the crystallized oligomer. For ITC, the full sequences are as follows: the H′ “top” sequence: 5′-GCCAAAAAAGCATTGCTTATCAATTTGTTGCACC-3′; the complentary H′ “bottom” sequence, 5′-GGTGCAACAAATTGATAAGCAATGCTTTTTTGGC-3′. Highly purified (2 HPLC purifications) DNA 34-mer strands for ITC studies were obtained from RNA-TEC (Belgium). RNA-TEC HPLC analysis indicated that each strand was > 95% pure, with trace amounts of both earlier- and later-eluting impurities.

HPLC-purified, 5′-fluorophore-labeled DNA 35-mer strands for FRET studies were obtained from Integrated DNA Technology (IDT). The oligonucleotides were identical to the ITC fragment except that the 5′ end was extended by one base (dT for the top strand, dC for the bottom strand) to avoid fluorophore quenching by terminal guanines. A 34 bp duplex was the product of annealing 35-mers each with one overhanging pyrimidine at the 5′ end, to which

the FRET donor (6-carboxyfluorescein (FAM)) and acceptor (tetramethylrhodamine (TAMRA)) were attached. The top strand FAM is linked to the 5′-deoxythymidine through a six carbon phosphoramidite linker; TAMRA is attached to the bottom strand 5′-deoxycytodine by the same linker. Except for the choice of overhanging pyrimidine on the bottom strand, the oligomer is identical in design to a fragment investigated previously by FRET.[14; 15] IDT HPLC analysis indicated that each strand was ≥ 95% pure and approximately 100% labeled with its fluorescent dye. The FRET top strand contains four additional negative charges (two from additional DNA phosphates, two from the fluorescein) relative to its ITC counterpart. The FRET bottom strand contains two additional negative charges relative to its ITC counterpart (from DNA phosphates; TAMRA is net neutral).

Duplex H′ was generated by mixing equimolar quantities of the complementary single strands, then incubating in a water bath at 85°C followed by overnight cooling. Typically the annealing of strands was 90 – 95% complete, as judged by HPLC analysis. The remaining 5 – 10% (probably unannealed strands) should not affect ITC and FRET since nonspecific binding (27; unpublished results). Concentrations of the ITC and FRET fragments were determined using molar extinction coefficients at 260 nm of $4.2 \times 10^5\ M^{-1}cm^{-1}$(27) and $4.8 \times 10^5\ M^{-1}cm^{-1}$ (calculated using the IDT values of $\varepsilon_{260,TAMRA} = 2.9 \times 104\ M^{-1}cm^{-1}$ and $\varepsilon_{260,FAM} = 2.1 \times 10^4\ M^{-1}cm^{-1}$), respectively.

Buffers

The buffer for all FRET and ITC binding studies was 0.010 M K_2HPO_4 (pH 8.3 at 20°C) and 0.001 M K_2EDTA. In experiments with KGlu, significant additions of potassium hydroxide (up to 0.02 M) were required to adjust the pH to 8.3, so that the $[K^+]$ concentration exceeded that of the anion of interest by up to 0.042 M at high $[Glu^-]$. In experiments with glycine betaine, the solute was added to a solution containing 0.26 M KCl. In FRET titrations, the buffer also contained 100 μg/mL BSA to minimize adsorption of IHF to the cuvette walls.

ITC Data Collection and Analysis

Almost all titrations reported here were obtained on a VPITC (Microcal, Inc). Normalized heat signals were calculated using the bundled Origin software. (A small number of experiments were performed with an earlier generation Omega ITC (Microcal, Inc) as indicated in Table 4.) Data were analyzed and plotted in Igor Pro 5/6.

An ITC titration includes heat contributions from ligand binding, ligand heat of dilution, as well as the mechanics of ligand addition. Subtraction of the baseline signal (the latter two contributions) was performed in one of two ways. For titrations in which the reaction was effectively completed early in the titration, the heat of macromolecule dilution was determined internally through back-extrapolation of the last 8–10 injections. In these cases, we verified that the protein heat of dilution was comparable to these baseline values in order to eliminate the the possibility of complications from nonspecific binding. In weaker binding titrations (0.22 M K^+ and above), a control titration of macromolecule into buffer was performed and subtracted from the binding titration.

Binding titrations were fit to a 1:1 binding model. ITC fits directly yield values for the standard enthalpy of binding $\Delta H°_{obs}$ and the binding constant K_{obs}. Standard free energy and entropy of binding are determined from $\Delta G°_{obs} = -RTlnK_{obs}$ and $\Delta S°_{obs} = (1/T)(\Delta H°_{obs} - \Delta G°_{obs})$. In all ITC studies, the starting concentration of the biopolymer in the cell was 5 – 25μM. At these concentrations, values of $K_{obs} \leq 3 \times 10^7\ M^{-1}$ appear to be accurately determined; if K_{obs} exceeds this value, it must be determined from the final 10% (or less) of the titration. This region of the titration may be disproportionately affected by the presence of DNA impurities

(e.g., imperfectly annealed strands and/or duplexes with one or more missing bases (failure sequences)).

IHF binds DNA nonspecifically at ≤ 0.1 M KCl with a small occluded site size of only 3 to 5 bp (27; KVM unpublished). At these low salt concentrations, nonspecific binding to the 34 bp specific H′ DNA fragment[27] and slow dissociation kinetics of specific complexes[9] complicate the analysis of reverse (DNA into IHF) titrations. Therefore, at or below 0.1 M K^+, only forward (IHF into DNA) ITC titrations were performed to determine $\Delta H°_{obs}$ (but not K_{obs}) for specific binding.

FRET Samples, Data Collection and Analysis

Samples—IHF and DNA samples for FRET measurements were dialyzed and concentrations determined spectrophotometrically at high concentration (≥ 10 μM IHF, 1.5 μM DNA); the samples were then diluted into eppendorf vials containing buffer and BSA to make FRET stock reagent solutions of ca. 1 μM. Lower concentrations of reagents were obtained from these stocks by serial dilution, using eppendorf vials that had been pre-incubated in buffer-BSA solution for ca.10 hours to reduce adsorption of IHF. (In our hands, IHF (and HU) adsorb more strongly to eppendorf vials than to quartz cuvettes (regardless of siliconization)). Samples for FRET measurements were prepared in the cuvette by adding buffer, then DNA, then protein, manually mixing for 15 seconds, and equilibrating for 3′ in the temperature-controlled fluorometer cell carriage. Thermal equilibrium was also achieved on this timescale, as determined in dummy runs using a thermocouple probe to measure the sample temperature. For both protein and solute titrations, a separate aliquot of both IHF and DNA was used for each point in the titration. In protein titrations, the DNA concentration in the cell was typically 35 nM. In “solute titrations”, IHF and H′ DNA were added at equimolar concentrations (typically 35 nM). The different salt concentrations in each sample were obtained by combining the appropriate volumes of a high salt and low salt buffer. Betaine titrations were performed similarly, using 0 M and 4 M Betaine buffers (in 0.26 M KCl).

Controls were performed to ensure that chemical equilibrium was achieved at each point. First, addition of unlabeled DNA to an already-equilibrated reaction mix, followed by manually mixing, re-equilibrated within the dead time of the measurement. This indicates relatively rapid on-off rates at these salt concentrations, as expected.[9; 14; 15] Thermodynamic stability of the dimer at the nM concentrations required for FRET was indicated by a lack of sigmoidicity in plots against total IHF concentration. Furthermore, an increase in the experimental concentration regime (using a 50-fold higher DNA concentration of 1.5 μM) had no effect on the measured K_{obs}. Controls were also performed to eliminate the possibility that the IHF heterodimer is metastable, in which case DNA binding would trap the dimeric state of the protein and prevent the observation of equilibrium. At various protein concentrations, the transfer efficiency did not change over a period of several hours. Changing the order of reagent addition (protein, then DNA) and/or allowing the protein to equilibrate at nM concentrations for up to one hour in the cuvette prior to addition of DNA had no effect on the FRET efficiency.

Data Collection—FRET experiments were performed in an L-shaped PTI (Photonic Technology Instruments) fluorometer, equipped with a Xe lamp and single monochromators on the excitation and emission beam path. Measurements were taken in a Starna 160 μL fluorometer cuvette using magic angle conditions. FRET intensity measurements were used to assay titrations of labeled H′ and H1 DNA with IHF, as well as titrations of IHF –H′ DNA mixtures with salts (KCl, KGlu) and the osmolyte glycine betaine.

Analysis of Protein Titrations—Binding isotherms in IHF (forward) titrations of DNA were obtained from the fractional change in TAMRA fluorescence. For our purposes, use of

this quantity was desirable because it normalizes the signal for DNA concentration, cuvette alignment and lamp intensity, reducing the noise in a titration. Using this approach, two emisson spectra were obtained at each point in the titration: one from 500 – 615 nm using an excitation wavelength of 490 nm; the other an excitation wavelength of 560 nm (a wavelength at which only TAMRA absorbs) and a wavelength range of 570 to 615 nm. The latter spectrum was used to normalize the sample signal intensity.

The fractional change in TAMRA fluorescence was calculated using the principles developed by Clegg as follows.[75] First, the portion of the 490 nm-excited spectrum due to TAMRA was isolated by subtracting a reference spectrum of DNA labeled with FAM only (see Figure 3 for spectra pre- and post- subtraction). Prior to subtraction, the reference spectrum was normalized to the fluorescence intensity of each FRET DNA spectra over the wavelength range where only FAM emits (510 – 530 nm). The resulting signal at each wavelength from 570 – 615 nm was divided by the signal at the corresponding wavelength from the spectrum obtained through excitation at 560 nm.

The resulting quotient at each wavelength is a ratio of the TAMRA fluorescence obtained primarily through energy transfer from FAM, to the TAMRA fluorescence obtained by direct excitation. This quantity, termed 'ratio$_A$' by Clegg (i.e., it is an 'acceptor ratio'),[75] has been used previously in binding assays. (In these cases, the observed ratio$_A$ was converted to an observed FRET efficiency prior to fitting.[7; 76; 77; 78]) Determinations of ratio$_A$ at each wavelength are equivalent mathematically,[75] so were averaged to reduce noise. The intrinsic magnitude of ratio$_A$ is a function of both the FRET efficiency and the extinction coefficients of the FRET pair.[75]

In protein titrations, we used the observed ratio$_A$ (ratio$_A^{obs}$) at each point in a protein titration as a binding signal. The fraction of H′ DNA molecules occupied by IHF, θ, is then determined according to

$$\theta = \frac{ratio_A^{obs} - ratio_A^{\min}}{ratio_A^{\max} - ratio_A^{\min}} \tag{9}$$

where ratio$_A^{min}$ and ratio$_A^{max}$ are empirically-determined values for ratio$_A$ of free DNA and IHF-bound DNA, respectively. For IHF titrations, values of ratio$_A^{min}$ (ca. 0.15) and ratio$_A^{max}$ (ca. 0.6) were determined by fitting. (This approach requires that the ratio of TAMRA extinction coefficients $\varepsilon_{490,TAMRA}/\varepsilon_{560,TAMRA}$ is the same in the free and bound states, which we verified).

Values of K_{obs} for each titration were calculated through iterative fitting using K_{obs} as a fit parameter. Equation 10 describes the dependence of θ values on K_{obs}

$$\theta = 1/2\left[(1 + \frac{[P]_{tot}}{[D]_{tot}} + \frac{1}{K_{obs}[D]_{tot}}) - \sqrt{(1 + \frac{[P]_{tot}}{[D]_{tot}} + \frac{1}{K_{obs}[D]_{tot}})^2 - 4[P]_{tot}}\right] \tag{10}$$

where $[P]_{tot}$ and $[D]_{tot}$ are the total IHF and DNA concentrations at each point in the titration. Each value listed in Table 2 represent the results of global fitting to all protein titrations at the given salt condition. The listed error shows the standard deviation in K_{obs} obtained from the individual datasets.

Analysis of FRET Solute Titrations—The quantities ratio$_A^{min}$ and ratio$_A^{max}$ may be a function of solute concentration. Therefore direct FRET solute titrations required separate determination of these quantities in order to generate an experimental upper and lower baseline.

The description of this determination follows and is illustrated in Supplementary Figure 1. Protein titrations at several solute concentrations were performed on the same day as the solute titration (an example titration set is provided in Supplementary Figure 1a). We find that $ratio_A^{min}$ is independent of solute concentration for all solutes examined by FRET, but that $ratio_A^{max}$ displays a slight dependence on [KGlu] and [KCl], but not [glycine betaine]. Over the range of [KGlu] examined (0.30 – 0.70 M), $ratio_A^{max}$ decreases by ca. 15%, as illustrated in Supplementary Figure 1a. Over the range of [KCl] examined (0.18 – 0.30 M), it decreases by 10 – 15%. The origin of this dependence is likely the [salt]-dependence of $\varepsilon_{FAM,490}$, which would impact $ratio_A^{max}$, but not $ratio_A^{min}$. We examined the [KGlu]-dependence of FAM fluorescence intensity and found it to change linearly on a semi-log plot, decreasing 25% over the range 0.16 to 0.80 M KGlu. Therefore, $ratio_A^{max}$ was obtained by interpolation to generate a full upper baseline (see dotted line in Supplementary Figure 1b).

In GB titrations, the activity of KCl is reduced by its preferential interaction with GB, thereby exerting a secondary and indirect effect on the stability of the IHF – H′ DNA complex. Using the analysis of Hong et al,[37] we corrected for this to calculate the effect of GB on ln K_{obs} at constant KCl activity

$$\left(\frac{\partial \ln K_{obs}}{\partial m_3}\right)_{a_4} = \left(\frac{\partial \ln K_{obs}}{\partial m3}\right)_{m_4} - \frac{S\,K_{obs}\Delta Osm_{34}}{2m_3m_4(1+\varepsilon_{\pm})_{m3}} \tag{11}$$

where components 3 and 4 are GB and KCl, respectively. For GB and KCl, a recent analysis has obtained $\Delta Osm_{34}/(m_3m_4) = -0.046\ M^{-1}$ (J Cannon, unpublished result), approximately half as large as the value previously reported.[37] $(1 + \varepsilon_{\pm})$ is a KCl molality-activity correction, equal to 0.89 at 0.26 M KCl. For KCl, $SK_{obs} = -8.8$, so that the final term in equation 11 is −0.23. Note that the Hong et al reference contains a typographical error in the sign of this term (equation (A6) in the original paper).

In solute titrations with KGlu and glycine betaine, the wavelength of maximum FAM emission was noticeably slightly blue-shifted at the highest concentrations. This effect was replicated in singly-labeled FAM-DNA conjugates, and FAM-only DNA spectra at the given solute concentration were used as the reference fluorescein signal in the subtraction step.

Structural Calculations

Figure 1 was generated using Pymol.[79] The structure is PDB code 1IHF[1] modified to incorporate the missing 3 C-terminal residues in IHF chain α using Modloop.[80] This modified structure was used to calculate the cationic and anionic composition of the interface.

Supplementary Material

Refer to Web version on PubMed Central for supplementary material.

References

1. Rice PA, Yang SW, Mizuuchi K, NAsh HA. Crystal structure of an IHF-DNA complex: A protein-induced DNA u-turn. Cell 1996;87:1295–1306. [PubMed: 8980235]
2. Friedman DI. Integration Host Factor - a Protein for All Reasons. Cell 1988;55:545–554. [PubMed: 2972385]
3. Nash, HA. The HU and IHF Proteins: Accessory Factors for Complex Protein-DNA Assemblies. In: Lin, ECC.; Lynch, AS., editors. Regulation of Gene Expression in Escherichia Coli. Chapman and Hall; New York: 1996. p. 149-179.

4. Johnson, RC.; Johnson, LM.; Schmidt, JW.; Gardner, JF. Major Nucleoid Proteins in the Structure and Function of the *Escherichia coli* Chromosome. In: Higgins, NP., editor. The Bacterial Chromosome. ASM Press; Washington, D.C: 2005. p. 65-132.
5. Ortega ME, Catalano CE. Bacteriophage lambda gpNu 1 and Escherichia coli IHF proteins cooperatively bind and bend viral DNA: Implications for the assembly of a genome-packaging motor. Biochemistry 2006;45:5180–5189. [PubMed: 16618107]
6. Azaro, MA.; Landy, A. Lambda integrase and the lambda Int family. In: Craig, NL.; Craigie, R.; Gellert, M.; Lambowitz, AM., editors. Mobile DNA II. ASM Press; Washington, D.C: 2002. p. 118-148.
7. Lorenz M, Hillisch A, Goodman SD, Diekmann S. Global structure similarities of intact and nicked DNA complexed with IHF measured in solution by fluorescence resonance energy transfer. Nucleic Acids Research 1999;27:4619–4625. [PubMed: 10556318]
8. Yang CC, Nash HA. The Interaction of Escherichia-Coli Ihf Protein with Its Specific Binding-Sites. Cell 1989;57:869–880. [PubMed: 2541927]
9. Dhavan GM, Crothers DM, Chance MR, Brenowitz M. Concerted binding and bending of DNA by Eschericia coli integration host factor. Journal of Molecular Biology 2002;315:1027–1037. [PubMed: 11827473]
10. Murtin C, Engelhorn M, Geiselmann J, Boccard F. A quantitative UV laser footprinting analysis of the interaction of IHF with specific binding sites: Re-evaluation of the effective concentration of IHF in the cell. Journal of Molecular Biology 1998;284:949–961. [PubMed: 9837718]
11. Aeling KA, Opel ML, Steffen NR, Tretyachenko-Ladokhina V, Hatfield GW, Lathrop RH, Senear DF. Indirect recognition in sequence-specific DNA binding by Escherichia coli integration host factor - The role of DNA deformation energy. Journal of Biological Chemistry 2006;281:39236–39248. [PubMed: 17035240]
12. Goodman SD, Velten NJ, Gao QA, Robinson S, Segall AM. In vitro selection of integration host factor binding sites. Journal of Bacteriology 1999;181:3246–3255. [PubMed: 10322029]
13. Wang SQ, Cosstick R, Gardner JF, Gumport RI. The Specific Binding of Escherichia-Coli Integration Host Factor Involves Both Major and Minor Grooves of DNA. Biochemistry 1995;34:13082–13090. [PubMed: 7548068]
14. Sugimura S, Crothers DM. Stepwise binding and bending of DNA by Escherichia coli integration host factor. Proceedings of the National Academy of Sciences of the United States of America 2006;103:18510–18514. [PubMed: 17116862]
15. Kuznetsov SV, Sugimura S, Vivas P, Crothers DM, Ansari A. Direct observation of DNA bending/unbending kinetics in complex with. DNA-bending protein IHF. Proceedings of the National Academy of Sciences of the United States of America 2006;103:18515–18520. [PubMed: 17124171]
16. Rivetti C, Guthold M, Bustamante C. Wrapping of DNA around the E. coli RNA polymerase open promoter complex. Embo Journal 1999;18:4464–4475. [PubMed: 10449412]
17. Craig ML, Suh WC, Record MT. Ho-Center-Dot and Dnase-I Probing of E-Sigma(70) Rna Polymerase-Lambda-P-R Promoter Open Complexes - Mg2+ Binding and Its Structural Consequences at the Transcription Start Site. Biochemistry 1995;34:15624–15632. [PubMed: 7495790]
18. Verhoeven EEA, Wyman C, Moolenaar GF, Hoeijmakers JHJ, Goosen N. Architecture of nucleotide excision repair complexes: DNA is wrapped by UvrB before and after damage recognition. Embo Journal 2001;20:601–611. [PubMed: 11157766]
19. Shi Q, Thresher R, Sancar A, Griffith J. Electron-Microscopic Study of (a)Bc Excinuclease - DNA Is Sharply Bent in the Uvrb DNA Complex. Journal of Molecular Biology 1992;226:425–432. [PubMed: 1386387]
20. Ruthenburg AJ, Graybosch DM, Huetsch JC, Verdine GL. A superhelical spiral in the Escherichia coli DNA gyrase A C-terminal domain imparts unidirectional supercoiling bias. Journal of Biological Chemistry 2005;280:26177–26184. [PubMed: 15897198]
21. Corbett KD, Shultzaberger RK, Berger JM. The C-terminal domain of DNA gyrase A adopts a DNA-bending beta-pinwheel fold. Proceedings of the National Academy of Sciences of the United States of America 2004;101:7293–7298. [PubMed: 15123801]

22. Kampranis SC, Bates AD, Maxwell A. A model for the mechanism of strand passage by DNA gyrase. Proceedings of the National Academy of Sciences of the United States of America 1999;96:8414–8419. [PubMed: 10411889]

23. Corbett KD, Schoeffler AJ, Thomsen ND, Berger JM. The structural basis for substrate specificity in DNA topoisomerase IV. Journal of Molecular Biology 2005;351:545–561. [PubMed: 16023670]

24. Tsodikov OV, Saecker RM, Melcher SE, Levandoski MM, Frank DE, Capp MW, Record MT. Wrapping of flanking non-operator DNA in lac repressor-operator complexes: implications for DNA looping. Journal of Molecular Biology 1999;294:639–655. [PubMed: 10610786]

25. Reijns M, Lu YJ, Leach S, Colloms SD. Mutagenesis of PepA suggests a new model for the Xer/cer synaptic complex. Molecular Microbiology 2005;57:927–941. [PubMed: 16091035]

26. Erzberger JP, Mott ML, Berger JM. Structural basis for ATP-dependent DnaA assembly and replication-origin remodeling. Nature Structural & Molecular Biology 2006;13:676–683.

27. Holbrook JA, Tsodikov OV, Saecker RM, Record MT. Specific and non-specific interactions of integration host factor with DNA: Thermodynamic evidence for disruption of multiple IHF surface salt-bridges coupled to DNA binding. Journal of Molecular Biology 2001;310:379–401. [PubMed: 11428896]

28. Kozlov AG, Lohman TM. Effects of monovalent anions on a temperature-dependent heat capacity change for Escherichia coli SSB tetramer binding to single-stranded DNA. Biochemistry 2006;45:5190–5205. [PubMed: 16618108]

29. Bujalowski W, Lohman TM. Negative Co-Operativity in Escherichia-Coli Single-Strand Binding Protein-Oligonucleotide Interactions.1. Evidence and a Quantitative Model. Journal of Molecular Biology 1989;207:249–268. [PubMed: 2661832]

30. Luger K, Mader AW, Richmond RK, Sargent DF, Richmond TJ. Crystal structure of the nucleosome core particle at 2.8 angstrom resolution. Nature 1997;389:251–260. [PubMed: 9305837]

31. Davey CA, Sargent DF, Luger K, Maeder AW, Richmond TJ. Solvent mediated interactions in the structure of the nucleosome core particle at 1.9 angstrom resolution. Journal of Molecular Biology 2002;319:1097–1113. [PubMed: 12079350]

32. Kozlov AG, Lohman TM. Calorimetric studies of E-coli SSB protein single-stranded DNA interactions. Effects of monovalent salts on binding enthalpy. Journal of Molecular Biology 1998;278:999–1014. [PubMed: 9600857]

33. Overman LB, Bujalowski W, Lohman TM. Equilibrium Binding of Escherichia-Coli Single-Strand Binding-Protein to Single-Stranded Nucleic-Acids in the (Ssb)65 Binding Mode - Cation and Anion Effects and Polynucleotide Specificity. Biochemistry 1988;27:456–471. [PubMed: 3280021]

34. Hong J, Capp MW, Anderson CF, Saecker RM, Felitsky DJ, Anderson MW, Record MT. Preferential interactions of glycine betaine and of urea with DNA: Implications for DNA hydration and for effects of these solutes on DNA stability. Biochemistry 2004;43:14744–14758. [PubMed: 15544345]

35. Cannon JG, Felitsky DJ, Record MT. Quantifying ion-specific Hofmeister interactions with protein surface. Biophysical Journal 2004;86:624a–624a.

36. Kontur WS, Saecker RM, Davis CA, Capp MW, Record MT. Solute probes of conformational changes in open complex (RPo) formation by Escherichia coli RNA polymerase at the lambda PR promoter: Evidence for unmasking of the active site in the isomerization step and for large-scale coupled folding in the subsequent conversion to RPo. Biochemistry 2006;45:2161–2177. [PubMed: 16475805]

37. Hong J, Capp MW, Saecker RM, Record MT. Use of urea and glycine betaine to quantify coupled folding and probe the burial of DNA phosphates in Lac repressor - Lac operator bindings. Biochemistry 2005;44:16896–16911. [PubMed: 16363803]

38. Felitsky DJ, Cannon JG, Capp MW, Hong J, Van Wynsberghe AW, Anderson CF, Record MT. The exclusion of glycine betaine from anionic biopolymer surface: Why glycine betaine is an effective osmoprotectant but also a compatible solute. Biochemistry 2004;43:14732–14743. [PubMed: 15544344]

39. Felitsky DJ, Record MT. Application of the local-bulk partitioning and competitive binding models to interpret preferential interactions of glycine betaine and urea with protein surface. Biochemistry 2004;43:9276–9288. [PubMed: 15248785]

40. Mascotti DP, Lohman TM. Thermodynamics of Single-Stranded Rna-Binding to Oligolysines Containing Tryptophan. Biochemistry 1992;31:8932–8946. [PubMed: 1382582]

41. Mascotti DP, Lohman TM. Thermodynamics of Single-Stranded Rna and DNA Interactions with Oligolysines Containing Tryptophan - Effects of Base Composition. Biochemistry 1993;32:10568–10579. [PubMed: 7691177]
42. Braunlin WH, Strick TJ, Record MT. Equilibrium Dialysis Studies of Polyamine Binding to DNA. Biopolymers 1982;21:1301–1314. [PubMed: 7115891]
43. Record MT, Lohman TM, Dehaseth P. Ion Effects on Ligand-Nucleic Acid Interactions. Journal of Molecular Biology 1976;107:145–158. [PubMed: 1003464]
44. Kozlov AG, Lohman TM. Stopped-flow studies of the kinetics of single-stranded DNA binding and wrapping around the Escherichia coli SSB tetramer. Biochemistry 2002;41:6032–6044. [PubMed: 11993998]
45. Ha JH, Capp MW, Hohenwalter MD, Baskerville M, Record MT. Thermodynamic Stoichiometries of Participation of Water, Cations and Anions in Specific and Nonspecific-Binding of Lac Repressor to DNA - Possible Thermodynamic Origins of the Glutamate Effect on Protein-DNA Interactions. Journal of Molecular Biology 1992;228:252–264. [PubMed: 1447786]
46. Barkley MD, Lewis PA, Sullivan GE. Ion effects on the lac repressor--operator equilibrium. Biochemistry 1981;20:3842–51. [PubMed: 7272280]
47. Roe JH, Record MT. Regulation of the Kinetics of the Interaction of Escherichia-Coli Rna-Polymerase with the Lambda-Pr Promoter by Salt Concentration. Biochemistry 1985;24:4721–4726. [PubMed: 2934084]
48. Revzin A, von Hippel PHV. Direct Measurement of Association Constants for Binding of Escherichia-Coli Lac Repressor to Non-Operator DNA. Biochemistry 1977;16:4769–4776. [PubMed: 20938]
49. Kowalczykowski SC, Lonberg N, Newport JW, von Hippel PH. Interactions of bacteriophage T4-coded gene 32 protein with nucleic acids. I. Characterization of the binding interactions. Journal of Molecular Biology 1981;145:75–104. [PubMed: 7265204]
50. Haseth PLD, Lohman TM, Burgess RR, Record MT. Nonspecific Interactions of Escherichia-Coli Rna-Polymerase with Native and Denatured DNA - Differences in Binding Behavior of Core and Holoenzyme. Biochemistry 1978;17:1612–1622. [PubMed: 350271]
51. Shkel IA, Ballin JD, Record MT. Interactions of cationic ligands and proteins with small nucleic acids: Analytic treatment of the large coulombic end effect on binding free energy as a function of salt concentration. Biochemistry 2006;45:8411–8426. [PubMed: 16819840]
52. Record MT, Zhang WT, Anderson CF. Analysis of effects of salts and uncharged solutes on protein and nucleic acid equilibria and processes: A practical guide to recognizing and interpreting polyelectrolyte effects, Hofmeister effects, and osmotic effects of salts. Advances in Protein Chemistry, Vol 51 1998;51:281–353.
53. Ballin JD, Shkel IA, Record MT. Interactions of the KWK6 cationic peptide with short nucleic acid oligomers: demonstration of large Coulombic end effects on binding at 0.1–0.2 M salt. Nucleic Acids Research 2004;32:3271–3281. [PubMed: 15205469]
54. Stigter D, Dill KA. Binding of ionic ligands to biopolymers. Abstracts of Papers of the American Chemical Society 1996;211:235-Coll.
55. Olmsted MC, Anderson CF, Record MT. Monte-Carlo Description of Oligoelectrolyte Properties of DNA Oligomers - Range of the End Effect and the Approach of Molecular and Thermodynamic Properties to the Poly-Electrolyte Limits. Proceedings of the National Academy of Sciences of the United States of America 1989;86:7766–7770. [PubMed: 2813356]
56. Fogolari F, Elcock AH, Esposito G, Viglino P, Briggs JM, McCammon JA. Electrostatic effects in homeodomain-DNA interactions. Journal of Molecular Biology 1997;267:368–381. [PubMed: 9096232]
57. Garcia-Garcia C, Draper DE. Electrostatic interactions in a peptide-RNA complex. Journal of Molecular Biology 2003;331:75–88. [PubMed: 12875837]
58. Misra VK, Honig B. On the Magnitude of the Electrostatic Contribution to Ligand-DNA Interactions. Proceedings of the National Academy of Sciences of the United States of America 1995;92:4691–4695. [PubMed: 7753866]
59. Sharp KA, Friedman RA, Misra V, Hecht J, Honig B. Salt Effects on Polyelectrolyte-Ligand Binding - Comparison of Poisson-Boltzmann, and Limiting Law Counterion Binding Models. Biopolymers 1995;36:245–262. [PubMed: 7492748]

60. Ma C, Baker NA, Joseph S, McCammon JA. Binding of aminoglycoside antibiotics to the small ribosomal subunit: a continuum electrostatics investigation. J Am Chem Soc 2002;124:1438–42. [PubMed: 11841313]
61. von Hippel PH, Wong KY. Neutral Salts: The Generality of Their Effects on the Stability of Macromolecular Conformations. Science 1964;145:577–580. [PubMed: 14163781]
62. Baldwin RL. How Hofmeister ion interactions affect protein stability. Biophysical Journal 1996;71:2056–2063. [PubMed: 8889180]
63. Courtenay ES, Capp MW, Saecker RM, Record MT. Thermodynamic analysis of interactions between denaturants and protein surface exposed on unfolding: Interpretation of urea and guanidinium chloride m-values and their correlation with changes in accessible surface area (ASA) using preferential interaction coefficients and the local-bulk domain model. Proteins-Structure Function and Genetics 2000:72–85.
64. Courtenay ES, Capp MW, Record MT. Thermodynamics of interactions of urea and guanidinium salts with protein surface: Relationship between solute effects on protein processes and changes in water-accessible surface area. Protein Science 2001;10:2485–2497. [PubMed: 11714916]
65. Pegram LM, Record MT Jr. Partitioning of atmospherically relevant ions between bulk water and the water/vapor interface. Proc Natl Acad Sci U S A 2006;103:14278–81. [PubMed: 16980410]
66. Pegram LM, Record MT Jr. Hofmeister salt effects on surface tension arise from partitioning of anions and cations between bulk water and the air-water interface. J Phys Chem B 2007;111:5411–7. [PubMed: 17432897]
67. Felitsky DJ, Record MT. Thermal and urea-induced unfolding of the marginally stable lac repressor DNA-binding domain: A model system for analysis of solute effects on protein processes. Biochemistry 2003;42:2202–2217. [PubMed: 12590610]
68. Mascotti DP, Lohman TM. Thermodynamic Extent of Counterion Release Upon Binding Oligolysines to Single-Stranded Nucleic-Acids. Proceedings of the National Academy of Sciences of the United States of America 1990;87:3142–3146. [PubMed: 2326273]
69. Mascotti DP, Lohman TM. Thermodynamics of oligoarginines binding to RNA and DNA. Biochemistry 1997;36:7272–7279. [PubMed: 9188729]
70. Record MT Jr, Anderson CF, Lohman TM. Thermodynamic analysis of ion effects on the binding and conformational equilibria of proteins and nucleic acids: the roles of ion association or release, screening, and ion effects on water activity. Quarterly Reviews of Biophysics 1978;11:103–78. [PubMed: 353875]
71. Tanford C. Extension of Theory of Linked Functions to Incorporate Effects of Protein Hydration. Journal of Molecular Biology 1969;39:539. [PubMed: 5357211]
72. Timasheff SN. Water as Ligand - Preferential Binding and Exclusion of Denaturants in Protein Unfolding. Biochemistry 1992;31:9857–9864. [PubMed: 1390769]
73. Parsegian VA. Solvation - Hopes for Hofmeister. Nature 1995;378:335–336.
74. Nash HA, Robertson CA, Flamm E, Weisberg RA, Miller HI. Overproduction of Escherichia-Coli Integration Host Factor, a Protein with Nonidentical Subunits. Journal of Bacteriology 1987;169:4124–4127. [PubMed: 3305480]
75. Clegg RM. Fluorescence Resonance Energy Transfer and Nucleic Acids. Methods In Enzymology 1992;211:353–388. [PubMed: 1406315]
76. Dragan AI, Read CM, Makeyeva EN, Milgotina EI, Churchill MEA, Crane-Robinson C, Privalov PL. DNA binding and bending by HMG boxes: Energetic determinants of specificity. Journal of Molecular Biology 2004;343:371–393. [PubMed: 15451667]
77. Clegg RM, Murchie AIH, Lilley DMJ. The Solution Structure of the 4-Way DNA Junction at Low-Salt Conditions - a Fluorescence Resonance Energy-Transfer Analysis. Biophysical Journal 1994;66:99–109. [PubMed: 8130350]
78. Dragan AI, Liu YY, Makeyeva EN, Privalov PL. DNA-binding domain of GCN4 induces bending of both the ATF/CREB and AP-1 binding sites of DNA. Nucleic Acids Research 2004;32:5192–5197. [PubMed: 15459288]
79. Delano WL. The PyMOL Molecular Graphics System. 2002
80. Fiser A, Sali A. ModLoop: automated modeling of loops in protein structures. Bioinformatics 2003;19:2500–2501. [PubMed: 14668246]

81. Raghunathan S, Kozlov AG, Lohman TM, Waksman G. Structure of the DNA binding domain of E-coli SSB bound to ssDNA. Nature Structural Biology 2000;7:648–652.

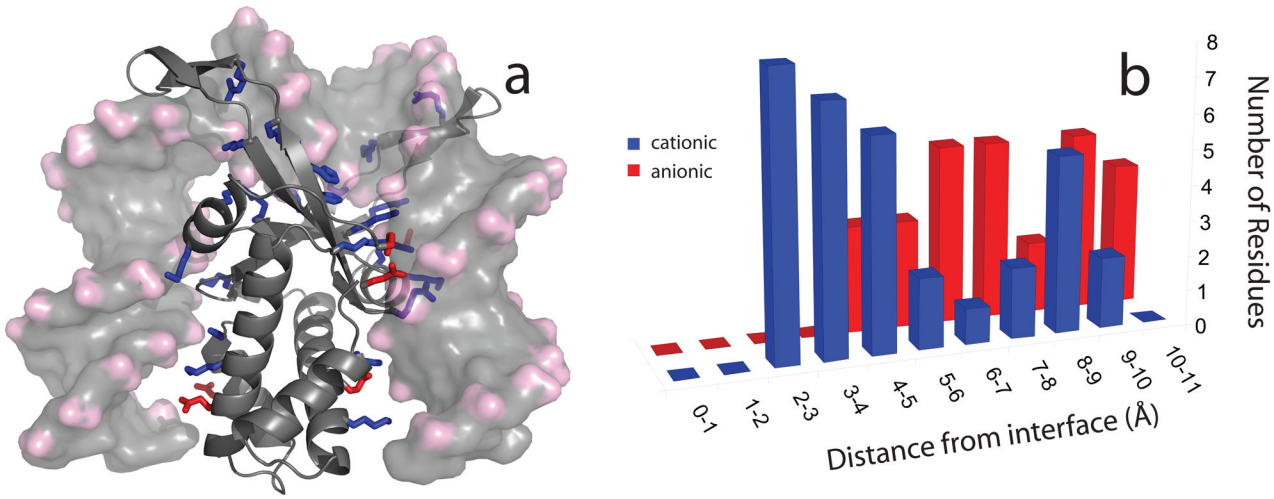

Figure 1.

Cationic and anionic residues in the IHF-H′DNA interface: (A) Positively charged functional groups of K, R, H side chains (blue) and negative carboxylate oxygens of D, E side chains (red) on IHF which are within 6 Å of an anionic DNA phosphate oxygen (pink) are highlighted. Calculations are from the coordinates of the crystal structure of the IHF – H′ DNA complex (PDB code 1IHF[1]). (B) Distribution of distances between each structural IHF charge (positive or negative) and the nearest anionic DNA phosphate oxygen. Structural IHF charges within 6 Å of an anionic DNA phosphate oxygen are considered to be part of the interface, together with the partner DNA phosphates.

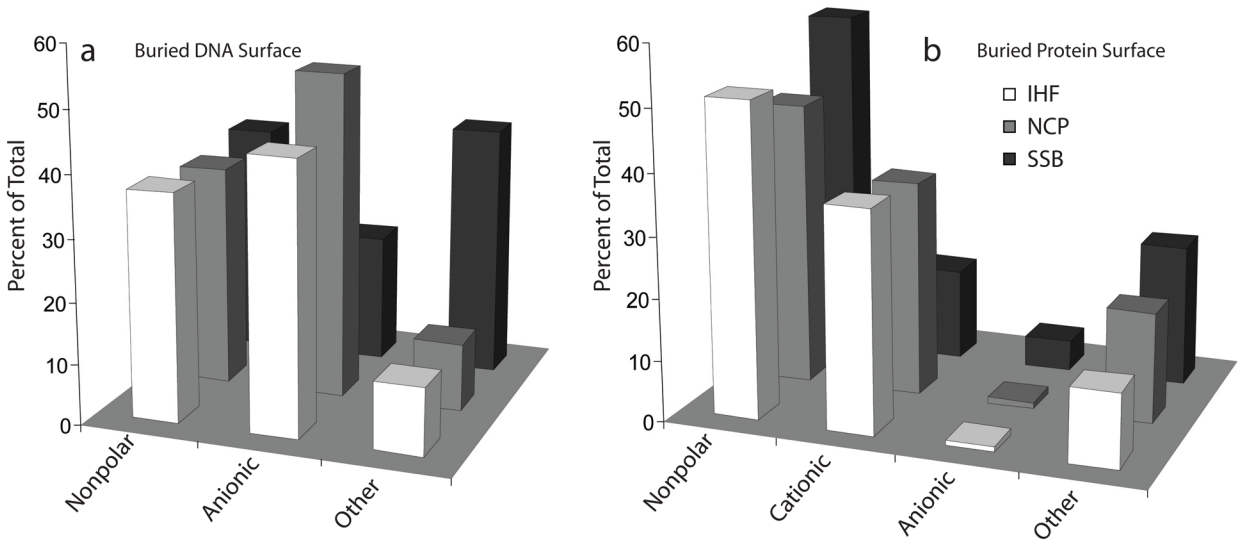

Figure 2.

Analysis of binding interfaces of wrapped DNA-protein complexes. The surface area buried from solvent (ΔASA) is broken down into percent contributions from nonpolar, cationic, anionic, and other polar surface for the (A) DNA and (B) protein. For the protein, cationic surface includes all guanidino, imino, and amino nitrogens and anionic surface includes all carboxylate oxygens. For DNA, anionic surface includes anionic DNA phosphate oxygens (2 anionic phosphate oxygens per phosphate group). IHF: IHF – H′ DNA complex (PDB code 1IHF[1]); NCP: nucleosome core particle – 147 bp DNA (PDB code 1KX5[31]); SSB: single-stranded DNA binding protein – 2 dC_{35} (PDB code 1EYG[81]).

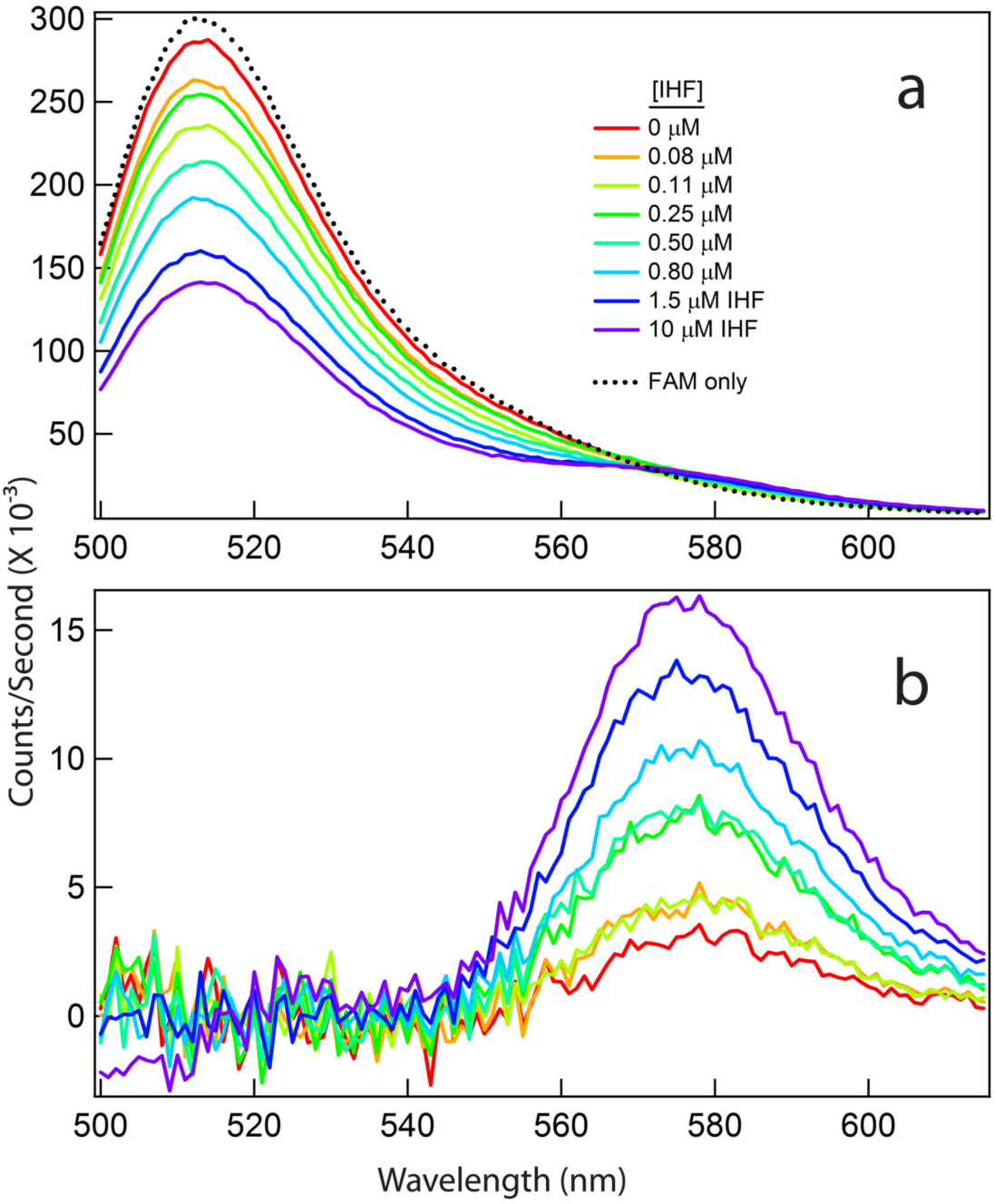

Figure 3.

Representative FRET data for H′ DNA – IHF interactions at 0.26 M KCl (0.282 M K^+, 20°C). (A) Representative fluorescence emission spectra of FAM-TAMRA labeled H′ DNA (200 nM) as a function of [IHF], plotted with a spectrum from a singly-labeled FAM-DNA conjugate. Excitation at 490 nm (maximum FAM absorbance). (B) Increased TAMRA fluorescence due to energy transfer from FAM to TAMRA, obtained by subtracting the intensity- normalized signal of 200 nM FAM-only H′ DNA from the spectra shown in panel A.

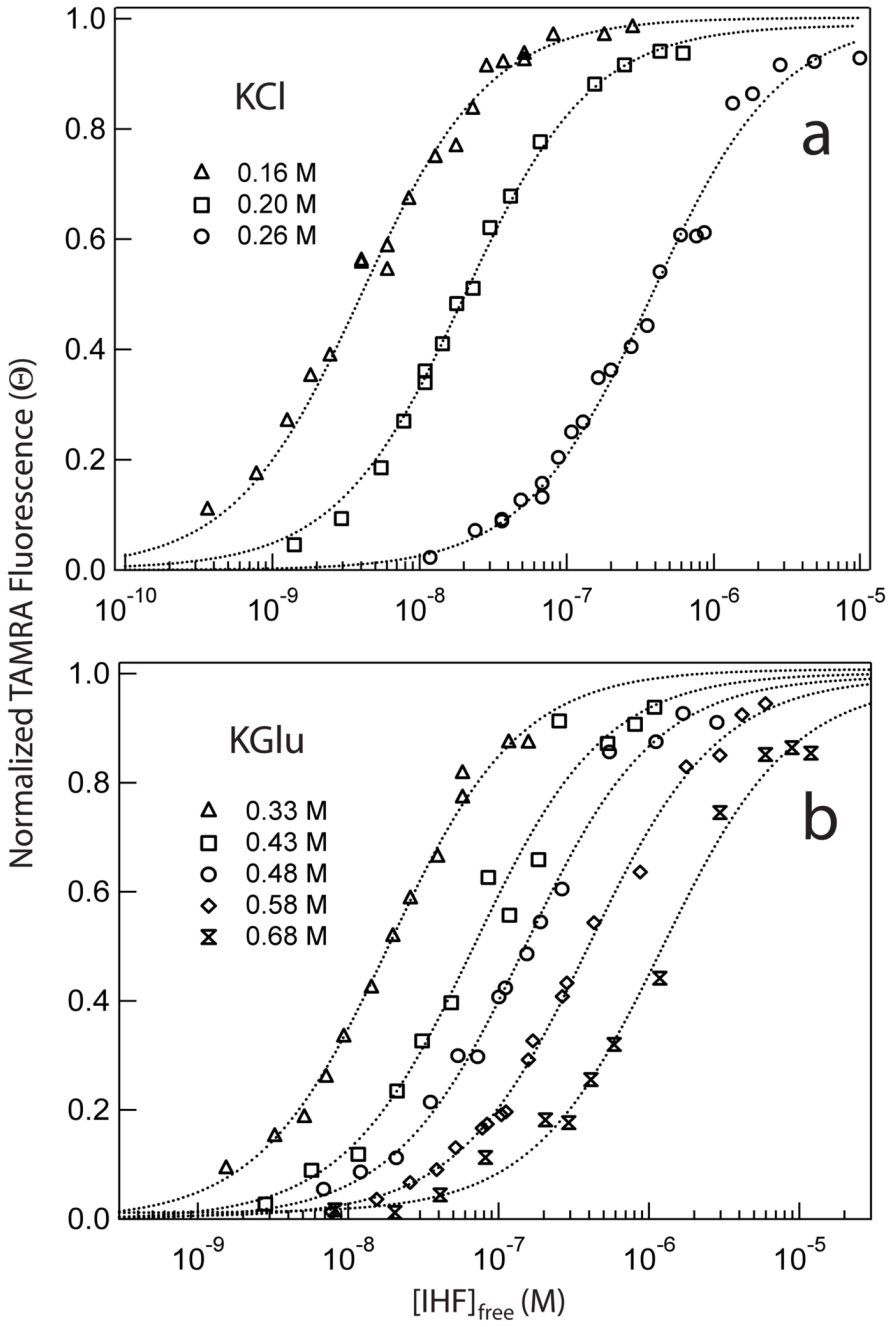

Figure 4.

Representative FRET-monitored IHF (forward) titrations of H′ DNA at 20°C, pH 8.3 at various KCl and KGlu concentrations: (A) Fractional change in TAMRA fluorescence (equal to θ, the fraction of H′ DNA molecules complexed with IHF) is plotted as a function of $[IHF]_{free}$ at 0.16 M KCl (open triangles), 0.20 M KCl (open squares), and 0.26 M KCl (open circles). (B) Normalized TAMRA fluorescence is plotted as a function of $[IHF]_{free}$ for binding to H′ DNA at 0.33 M KGlu (open triangles), 0.43 M KGlu (open squares), 0.48 M KGlu (open circles), 0.58 M KGlu (open diamonds), and 0.68 M KGlu (open ribbons).

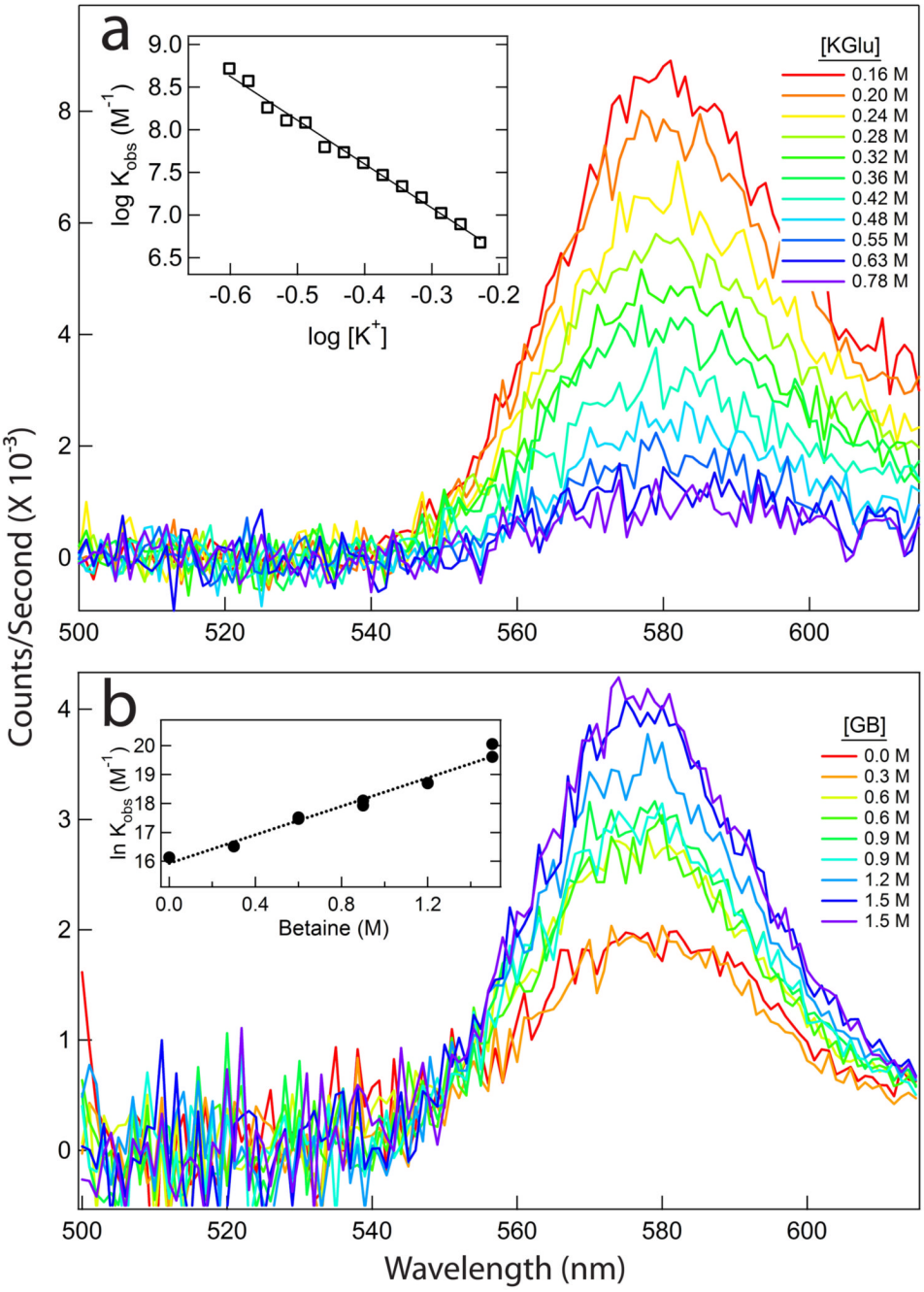

Figure 5.

FRET-monitored solute titrations of IHF-H′DNA complexes at 20°C, pH 8.3 (A) Representative “salt-back” titration. A family of TAMRA emission spectra for titration with KGlu of a 1:1 mixture of IHF and H′ DNA (each 35 nM) initially at 0.16 M KGlu (top spectrum). The inset plots the logarithm of the observed binding constant (log K_{obs}) versus the logarithm of K^+ concentration for the most accurate binding data ($0.1 < \theta < 0.9$; obtained for 0.25 M < [KGlu] < 0.59 M). A linear fit to the data yields a log-log slope of -5.1 ± 0.2. (B) Representative glycine betaine (GB) titration. TAMRA emission spectra for a titration of a 1:1 mixture of IHF and H′ DNA (each 50 nM) with GB at 0.26 M KCl, 20°C. The inset shows a semi-log plot of binding constants K_{obs} obtained from these data as a function of molar GB concentration (for

the data in the figure, the slope is 2.6 ± 0.2, and the intercept is 15.8 ± 0.2). Maximum intensities differs in Figures A and B differ because of differences in monochromator slit settings and lamp intensities.

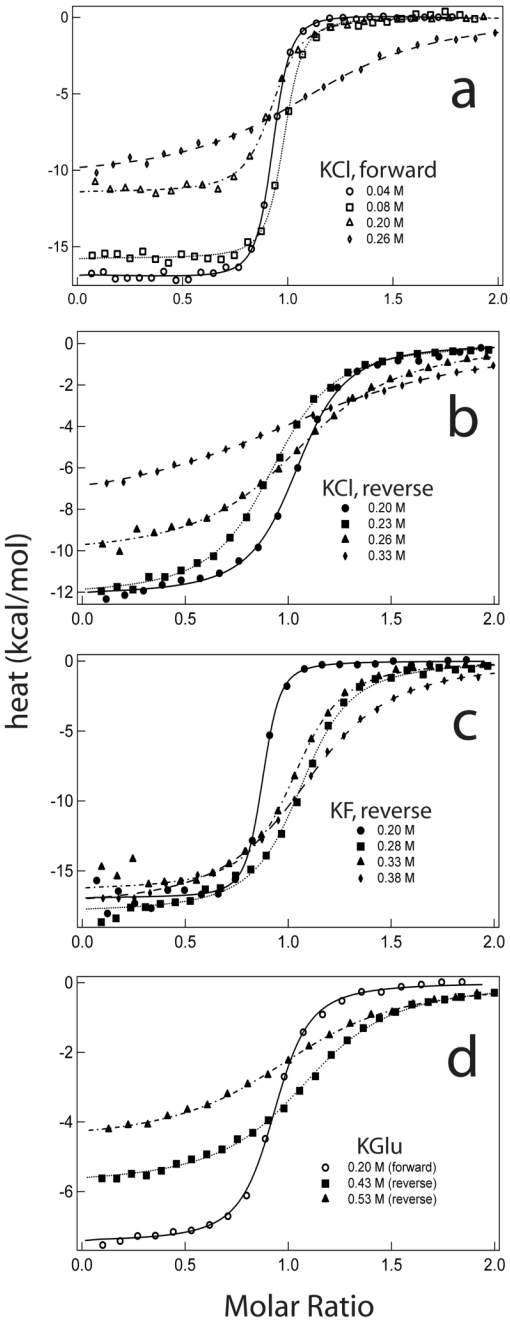

Figure 6.

Representative binding isotherms at 20°C for IHF-H′ DNA interactions obtained by isothermal titration calorimetry (ITC) as a function of salt concentration and the identity of the salt anion. (A) Forward (IHF into DNA) titrations in KCl; (B) reverse (H′DNA into IHF) titrations in KCl; (C) reverse titrations in KF; and (D) forward and reverse titrations in KGlu.

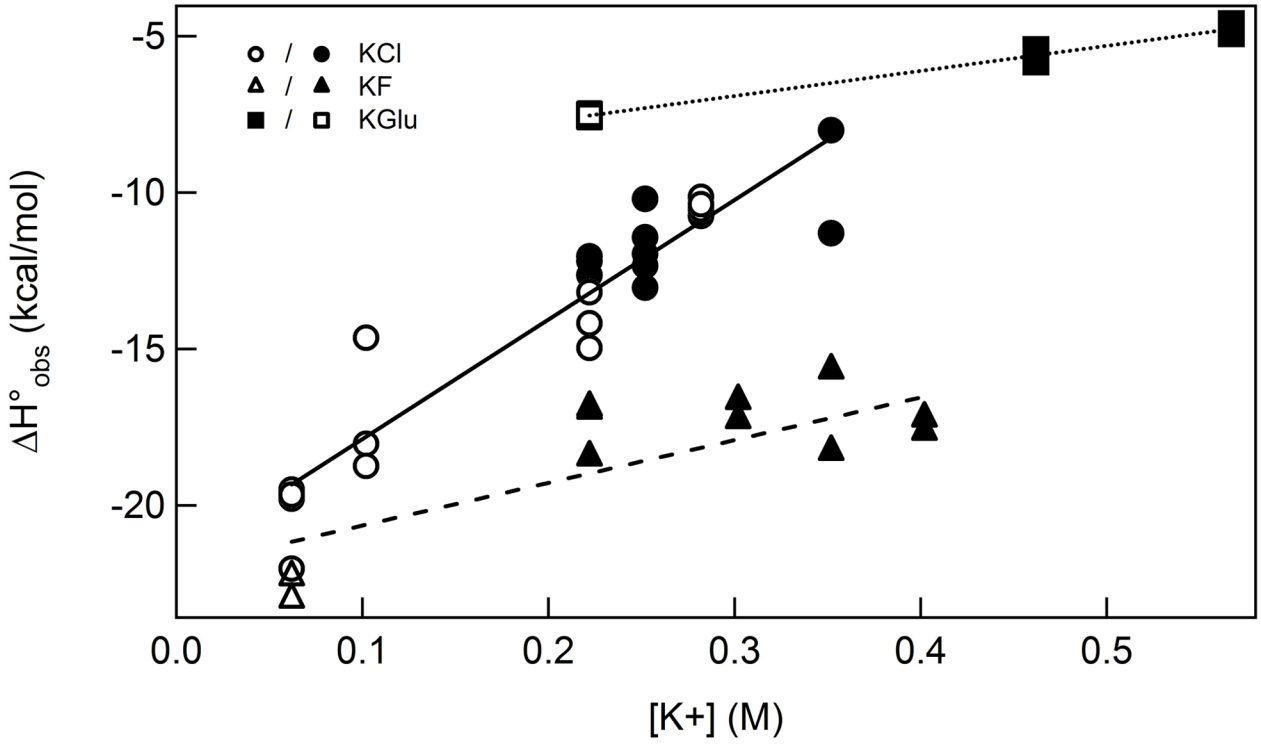

Figure 7.
ITC-determined binding enthalpies ΔH°_{obs} for formation of specific IHF-H′DNA complexes in KCl, KGlu, and KF as a function of $[K^+]$ in KCl (circles), KF (triangles) and KGlu (squares). Forward titrations are plotted as open symbols and reverse titrations as closed symbols. Results of all experiments are plotted; fitting errors for each experiment are far less than the scatter of repeat determinations and are not shown.

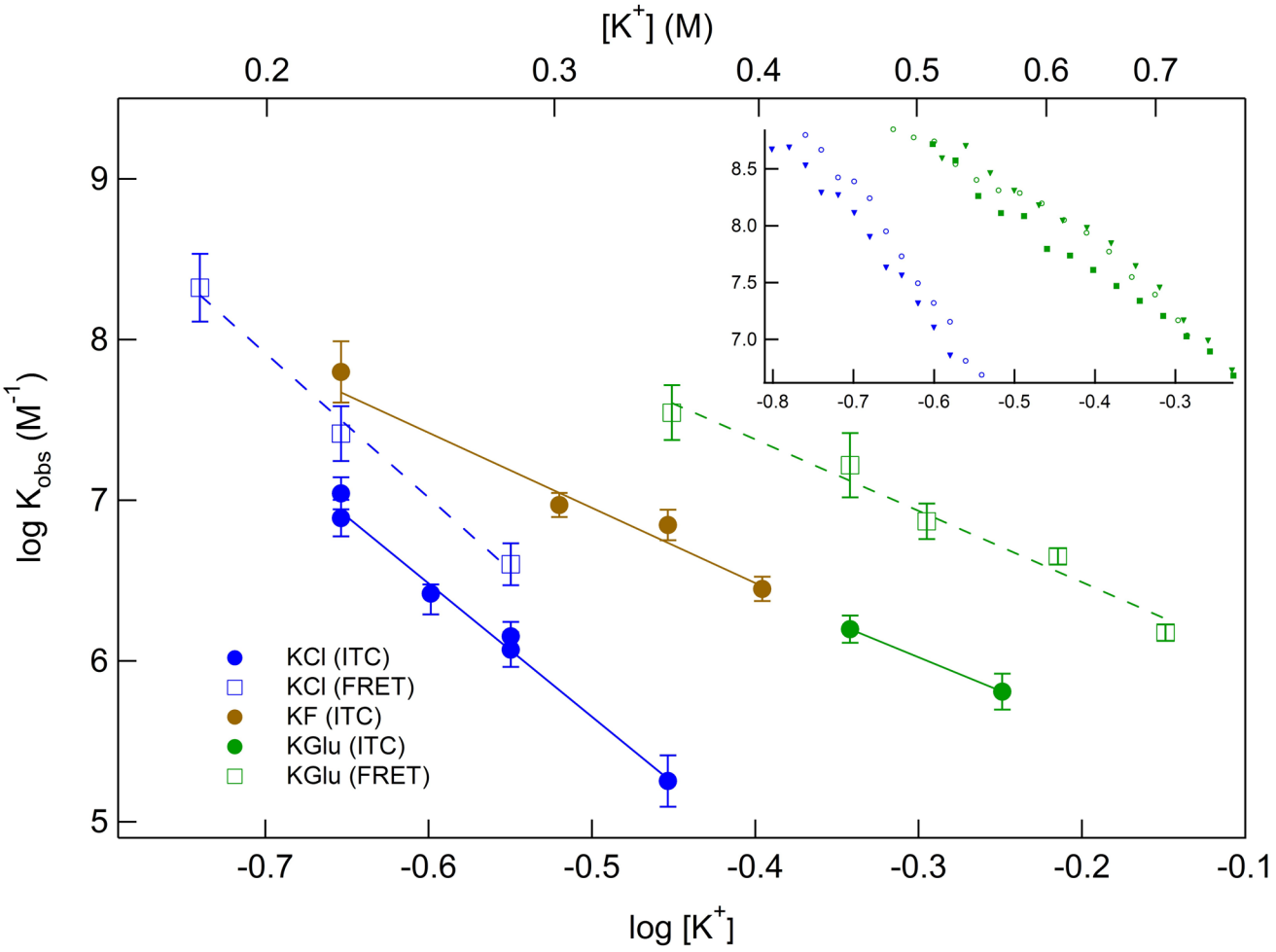

Figure 8.

Log-log plot of IHF-H′ ′DNA binding constants (K_{obs}) as a function of [K^+] determined either by FRET-detected forward titrations of 34 bp H′DNA (fluorophore labels covalently attached via one-base 5′ overhangs; see Methods) (open squares) or by ITC forward and reverse titrations using unlabeled, blunt-ended H′ DNA oligomers (solid circles; see Methods). K_{obs} data obtained in KCl (blue), in KF (brown), and in KGlu (green). Inset plots values of log K_{obs} from FRET-monitored salt-back titrations in KCl (blue) and in KGlu (green); different experiments with the same salt are indicated with different symbols in the same color.

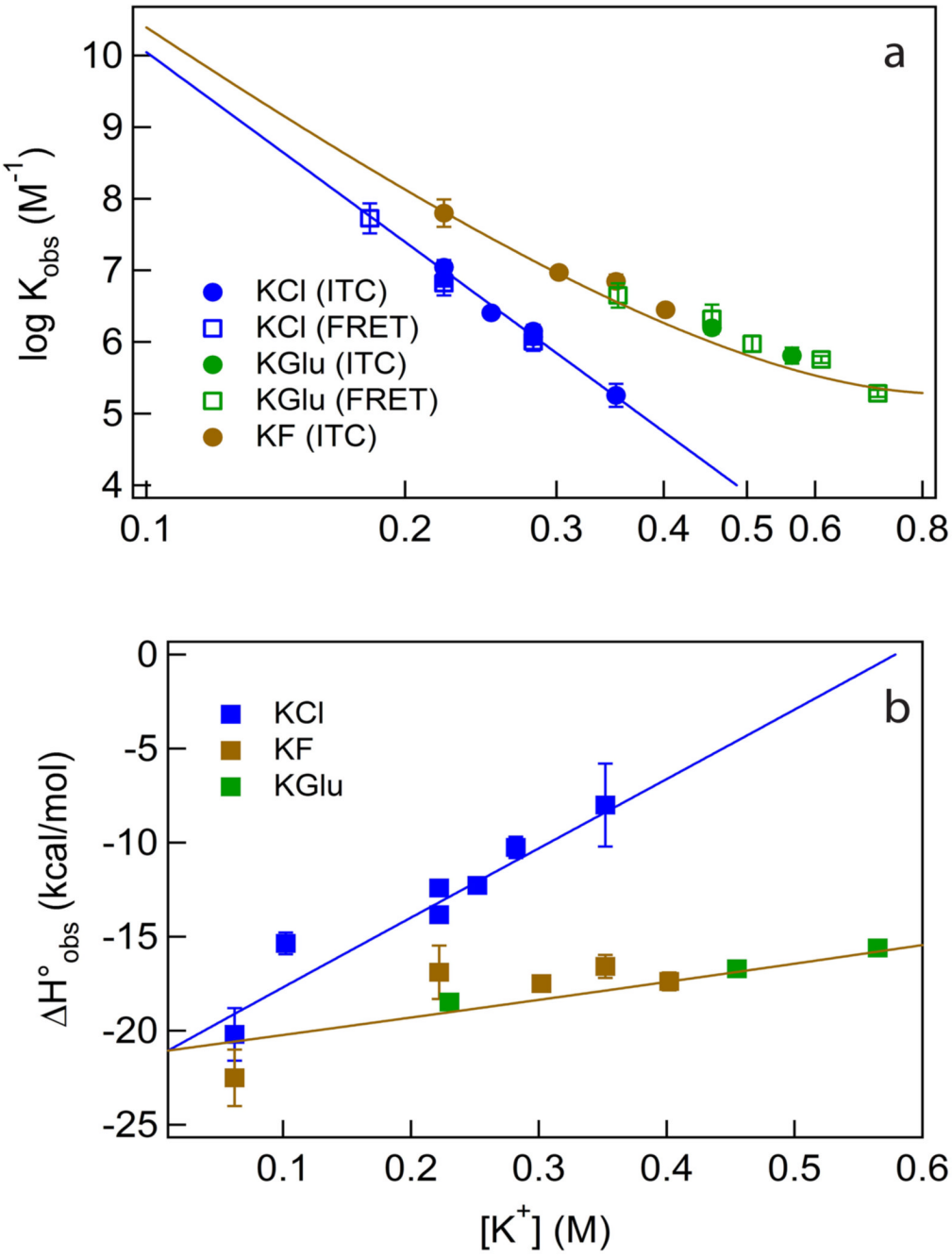

Figure 9.

Analyses of log K_{obs} and $\Delta H°_{obs}$ of IHF-H′DNA binding in terms of coulombic, Hofmeister, and osmotic effects of KCl, KF and KGlu. (A) Analysis of log K_{obs} (or $\Delta G°_{obs}$). FRET- and ITC-determined binding constants (see Fig. 8) are plotted as a function of $[K^+]$ by subtracting the systematic offset caused by chemical differences in the H′DNA oligonucleotides (see Discussion). The plotted curves are obtained from equation 6 which quantifies the coulombic, Hofmeister, and osmotic effects of these salts on log K_{obs} using the constraints described in the text and the values of the parameters listed in Table 5. (B) Analysis of $\Delta H°_{obs}$. ITC-determined binding enthalpies obtained from the data of Figure 7 by correction for the enthalpy of deprotonation of KGlu are plotted vs K^+ concentration. The plotted lines are obtained from

equation 7 quantifying Hofmeister contributions to the enthalpy using the same parameters as in Figure 9A, and tabulated in Table 5.

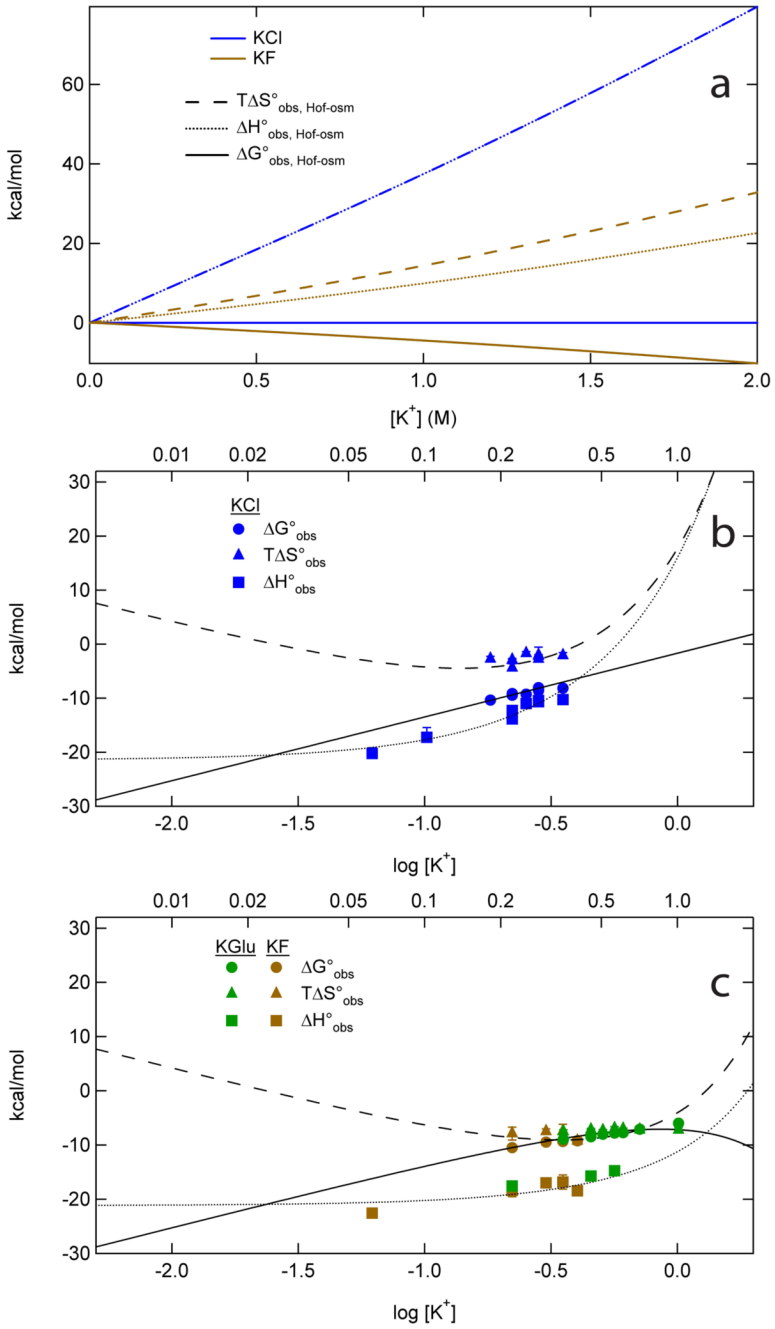

Figure 10.

SPM extrapolations to high and low concentrations of $[K^+]$. (A) Hofmeister and osmotic (Hof-osm) contributions $\Delta G°_{Hof\text{-}osm}$ (solid line), $T\Delta S°_{Hof\text{-}osm}$ (dashed line) and $\Delta H°_{Hof\text{-}osm}$ (dotted line) for KCl and KF/KGlu using values of K_p and $\Delta H°_p$ in Table 5. The quantities are plotted versus $[K^+]$, demonstrating the linear relationship between the Hofmeister-osmotic terms and [salt], as well as the partial (KGlu/KF) or full (KCl) compensation between enthalpic and entropic Hof-osm contributions to $\Delta G°_{obs}$. (B) and (C) display the predicted behavior of IHF – H′ DNA binding thermodynamics at high and low [salt] for KCl (B) and KF/KGlu (C). Solid lines, dashed lines, and dotted lines show the extrapolation of $\Delta G°_{obs}$, $T\Delta S°_{obs}$, and $\Delta H°_{obs}$,

respectively. The data are represented using the color scheme of Figures 8 and 9, except that no distinction is made betweenFRET and ITC data.

Table 1

Interfaces of Wrapped Protein-DNA Complexes

	Buried Surface Area (|ΔASA|) (Å^2)			Interface (6 Å) Charge Composition		
				DNA [d]	Protein[e]	
	Complex	DNA	Protein	Phosphates	Cationic	Anionic
IHF-H′DNA[a]	5,340	2,670	2,670	21	24	4
Nucleosome-DNA[b]	21,750	11,409	10,340	111	106	9
SSB- 2dC$_{35}$ [c]	13,000	7,110	5,890	31	27	10

[a] PDB file 1IHF;

[b] PDB file 1KX5;

[c] PDB file 1EYG

[d] Number of cationic and anionic residues within 6 Å of a DNA phosphate

[e] Number of DNA phosphates within 6 Å of a protein cationic residue

Table 2

IHF – H′ DNA Binding Constants by FRET

Salt	No. Expts	K_{obs} (M^{-1})
0.16 M KCl	5	2.1 (± 1.0) × 10^8
0.20 M KCl	5	2.6 (± 1.0) × 10^7
0.26 M KCl	3	4.0 (± 1.2) × 10^6
0.33 M KGlu	4	3.5 (± 1.8) × 10^7
0.43 M KGlu	3	1.7 (± 0.8) × 10^7
0.48 M KGlu	4	7.4 (± 1.8) × 10^6
0.58 M KGlu	5	4.5 (± 0.4) × 10^6
0.68 M KGlu	3	1.5 (± 0.1) × 10^6

Table 3

Salt-Dependences (SK_{obs}) of IHF-H′ DNA Binding

Salt	Method	[Salt] Range[a]	SK_{obs}	$K_{obs,X^-}/K_{obs,Cl^-}$ (0.33 M)b
KCl	ITC	0.20 – 0.33 M	−8.3 ± 1.0	1
KCl	FRET	0.16 – 0.26 M	−9.1 ± 1.6	1
KCl	FRET SB	0.18 – 0.28 M	−9.0 ± 1.2	1
KF	ITC	0.20 – 0.38 M	−4.7 ± 1.0	39
KGlu	ITC	0.43 – 0.53 M	−4.2 ± 1.8	29*
KGlu	FRET	0.33 – 0.68 M	−4.6 ± 0.9	58*
KGlu	FRET SB	0.25 – 0.58 M	−5.0 ± 1.0	86*

SB = salt-back

[a] The [salt] range over which the experimental data were obtained

[b] The measured K_{obs}, relative to the value in KCl (by the same method)

* Obtained by extrapolation to 0.33 M

Table 4

IHF-H′ DNA Binding Parameters by ITC

Salt	Direction	No. Expts	K_{obs} (M^{-1})	$\Delta H°_{obs}$ (kcal/mol)	$T\Delta S°_{obs}$ (kcal/mol)
0.04 M KCl	Forward	3	N/D	−20.2 ± 1.5	N/D
0.08 M KCl	Forward	2	N/D	−15.4 ± 0.6	N/D
0.20 M KCl	Forward	3	1.1 (± 0.3) × 10^7	−13.8 ± 0.4	−4.3 ± 0.4
0.20 M KCl	Reverse	3[a]	7.8 (± 2.3) × 10^6	−12.4 ± 0.4	−3.1 ± 0.5
0.23 M KCl	Reverse	5	2.6 (± 0.3) × 10^6	−10.7 ± 0.5	−2.0 ± 0.3
0.26 M KCl	Forward	3	1.4 (± 0.3) × 10^6	−10.3 ± 0.5	−1.9 ± 0.5
0.26 M KCl	Reverse	1	1.2 (± 0.3) × 10^6	−10.3 ± 0.6	−2.1 ± 0.6
0.33 M KCl	Reverse	2	1.8 (± 0.8) × 10^6	−9.4 ± 2.4	−2.4 ± 2.8
0.04 M KF	Forward	2	N/D	−22.5 ± 1.5	N/D
0.20 M KF	Reverse	3	6.3 (± 3.5) × 10^7	−16.9 ± 1.4	−6.4 ± 1.5
0.28 M KF	Reverse	2	9.3 (± 1.8) × 10^6	−17.5 ± 0.4	−8.1 ± 0.4
0.33 M KF	Reverse	2[a]	7.0 (± 1.7) × 10^6	−16.6 ± 0.6	−7.4 ± 0.6
0.38 M KF	Reverse	2	2.8 (± 0.5) × 10^6	−17.4 ± 0.5	−8.6 ± 0.5
0.20 M KGlu	Forward	2	N/D	−7.5 ± 0.2	N/D
0.43 M KGlu	Reverse	2	1.6 (± 0.4) × 10^6	−5.7 ± 0.2	2.6 ± 0.3
0.53 M KGlu	Reverse	2	6.5 (± 1.9) × 10^5	−4.7 ± 0.3	3.1 ± 0.3

[a] One experiment at this condition was performed using an Omega ITC.

Table 5

Salt Partitioning Model Parameters

Salt Ion	K_p (20°C)	$\Delta H°_{obs,p}$ (20°C) (kcal) [a]	$T\Delta S°_{obs,p}$ (20°C) (kcal) [a]
Potassium	[1.0]	−1.3	1.3
Chloride	[1.0]	−1.0	1.0
Fluoride	0.44	1.6	1.1
Glutamate	0.44	1.6	1.1

[ ] = parameters fixed; parameters describing the interface magnitude and coulombic contribution to the [salt]-dependence were also fixed at $\Delta B_{H_2O} = -1000$, $SK_{obs,coul} = -8.8$.

[a] Representative Set